Final Report Number
110-58

Submitted to
National Aeronautics and Space Administration
Washington, D. C.

BUREAU OF ENGINEERING RESEARCH

Final Report

DYNAMIC ANALYSIS OF STABILITY AND DEPLOYMENT OF INFLATABLE SHELL STRUCTURES

by

Dr. Thomas E. Falgout
Assistant Professor of
Engineering Mechanics

and

Dr. George E. Weeks
Assistant Professor of
Aerospace Engineering

Contract No. NAS8-21480
Control No. DCN1-8-75-0012 (IF)

Revised January 1970

BER

COLLEGE OF ENGINEERING

THE UNIVERSITY OF ALABAMA 1831

UNIVERSITY OF ALABAMA

UNIVERSITY ALABAMA

University Account No.
22-6585

DYNAMIC ANALYSIS OF STABILITY AND DEPLOYMENT OF INFLATABLE SHELL STRUCTURES

FINAL REPORT
Contract No. NAS-8-21480
Control No. DCN1-8-75-0012 (IF)

Dr. Thomas E. Falgout
Assistant Professor of
Engineering Mechanics

and

Dr. George E. Weeks
Assistant Professor of
Aerospace Engineering

University of Alabama
Bureau of Engineering Research
University, Alabama

December 15, 1969 (revised)

Contents

Pages

Introduction..... iii

Chapter I - Vibrations of Pressurized Membrane Cylindrical Shells

A. Introduction..... 1

B. Analysis..... 2

Chapter II - Vibrations of Inflated Cylindrical Beams

A. Introduction..... 19

B. Analysis..... 20

Chapter III - Dynamic Response of Rods Subjected to Gyroscopic Motion

A. Introduction..... 34

B. Analysis..... 35

Chapter IV - Vibration of Rods Subjected to Gyroscopic Motion

A. Introduction..... 60

B. Analysis..... 61

Chapter V - Experimental Results

A. Flexible Rods..... 87

B. Inflatable Structures..... 91

Report Distribution..... 99

Introduction

The investigations reported here all fall within the guidelines of the objectives as delineated in NASA Contract NAS 8-21480. The primary structures analysed were inflated cylindrical shells, considered the most feasible configuration for use as space vehicle antennas and gravity-gradient damper booms. For the inflated membrane cylindrical shell the following investigations were performed.

The vibrational analysis of general pressurized cylindrical shells utilizing nonlinear membrane shell theory is presented. First order effects of stretching of the middle surface are included. The results are presented in a graphical form showing the variation in frequency for various internal pressure levels. A comparison of results with a known classical solution provided a check for the method of solution used:

The free vibration of long cantilevered cylindrical beams is considered. The effects of internal pressurization and transverse shear stiffness are included. The results are presented in a graphical form with a nondimensional frequency plotted against a nondimensional parameter which was a function of the shell shear stiffness and the internal pressure.

The nonlinear analysis of an inflated cylindrical beam with undeformed axis inclined at acute angles relative to the vertical and rotated uniformly about the vertical is presented. Steady state deflections are determined for flexible rods numerically

and compared to experimental deflection curves. From a steady state deflection or prestressed state a set of linear perturbation equations are derived. These equations are solved numerically for the natural frequencies associated with the perturbed motion. The results of these studies are presented and discussed in the latter parts of Chapter III and IV.

Experiments were designed and performed to check the theory and analytical results obtained. A detailed discussion of these experiments is included.

A brief summary is given at the beginning of each chapter. The notation and symbols used in each chapter are defined when introduced and may not be the same in the different chapters.

CHAPTER I

VIBRATIONS OF PRESSURIZED MEMBRANE CYLINDRICAL SHELLS

Summary

Nonlinear equations of motion are derived for a pressurized membrane cylindrical shell. The equations of motion are solved in closed form under the assumption of infinitesimal time dependent perturbations about the axisymmetric prestress state. Nondimensional natural frequencies are determined as a function of the number of half waves in the circumferential and meridional directions for various values of the internal pressure and shell geometry.

I-A Introduction

The investigation of the vibrations of prestressed shells requires a consideration of the nonlinear shell equations. The object of this chapter is to derive and solve the equations governing the vibrational behavior of prestressed membrane cylindrical shells. Using the nonlinear membrane shell theory of reference (I-1) the vibrational analysis for simply supported cylindrical shells is determined.

The effect of internal pressurization is accurately accounted for by permitting the pressure force to always remain normal to the deformed surface. In addition, first order effects of stretching of the "middle surface" of the membrane are included. The prestressed state of the shell is assumed to be satisfactorily given by the membrane state of stress.

Results are presented in a graphical form showing the variation of natural frequencies with internal pressure and shell dimensions for different wave numbers in the circumferential

and meridional directions. A comparison between frequencies obtained in this analysis and those obtained from other analyses appearing in the literature is included.

I-B Analysis

The shell geometry is illustrated in Figure 1. A point on the surface of the shell is located by the axial, circumferential, and radial coordinates (ξ,θ,r) respectively. The displacements of this point are (U,V,W) in the axial, circumferential, and radial directions respectively. The shell is assumed to be isotropic and homogeneous with a constant thickness h, Youngs modulus E, Poisson's ratio μ, and mass density ρ.

Governing Nonlinear Equations

The nonlinear equations for the cylindrical shell are derived from Hamilton's principle

$$\delta K = \int_{t_0}^{t} (\delta T + \delta \overline{W} - \delta \overline{U})\, dt \qquad (1)$$

where T is the kinetic energy of the system, $\overline{W}$ is the work done by the external loads, and $\overline{U}$ is the change in strain energy stored in the shell during deformation.

Kinetic energy. For this analysis, the inertia of the pressurizing gas will be neglected so that the kinetic energy for the membrane is

$$T = \frac{\rho h}{2} \int_A (\dot{U}^2 + \dot{V}^2 + \dot{W}^2)\, dA \qquad (2)$$

where dots over the symbols indicate differentiation with respect to time.

Virtual work of external loads. In deriving the expression for the virtual work of the external loads, it is assumed that the pressure force remains everywhere normal to the deformed surface. Thus the additional components of the force vector in the axial and circumferential directions must be included. With these considerations, the virtual work of the pressure loading is

$$\delta\bar{W} = \int_A p(-W_{,\xi})\, \delta U\, dA + \int_A p(-\frac{1}{r} W_{,\theta} + \frac{V}{r})\, \delta V\, dA + \int_A p(1 + U_{,\xi} + \frac{V_{,\theta}}{r} + \frac{W}{r})\, \delta W\, dA \qquad (3)$$

where $dA = r d\theta\, d\xi$ and commas denote differentiation with respect to the following subscripted variable. The first term in equation (3) is the component of the pressure loading in the axial direction, the second term is the component in the circumferential direction, and the third term is the component in the radial direction. Note that for the force component in the radial direction, the coefficient of $\delta\bar{W}$ has been appropriately modified to include the first order stretching effect of the "middle" surface. As a result, each of the terms in equation (3) are of first order in the displacements.

Strain Energy. Consistent (see for instance, (I-1) with the previously derived equations for the virtual work, the variation of the strain energy stored in the membrane is

$$\delta U = \int_A (N_\xi \delta\varepsilon_\xi + N_\theta \delta\varepsilon_\theta + N_{\xi\theta} \delta\varepsilon_{\xi\theta})\, dA \qquad (4)$$

where N_ξ, N_θ, and $N_{\xi\theta}$ are the stress resultants and ε_ξ, ε_θ, $\varepsilon_{\xi\theta}$ are the tensor components of strain to be developed in the next section.

Strain displacement relations. The nonlinear tensor components of strain, in terms of displacements, for a cylindrical coordinate system are from Reference (I-2)

$$\varepsilon_\xi = U_{,\xi} + \frac{1}{2}(U_{,\xi}^2 + V_{,\xi}^2 + W_{,\xi}^2)$$

$$\varepsilon_\theta = \frac{1}{r}\left[V_{,\theta} + W + \frac{1}{2r}(V_{,\theta} + W)^2 + \frac{1}{2r}(W_{,\theta} - V)^2 + \frac{1}{2r}(U_{,\theta})^2\right] \qquad (5)$$

$$\varepsilon_{\xi\theta} = \frac{U_{,\theta}}{r} + V_{,\xi} + \frac{1}{r} U_{,\xi} U_{,\theta} + \frac{1}{r} V_{,\xi}(V_{,\theta} + W) + \frac{1}{r} W_{,\xi}(W_{,\theta} - V)$$

Equations of motion. The nonlinear equations of motion and the corresponding boundary conditions of the cylindrical membrane are now obtained by substituting equations (2), (3), and (4) into equation (1) and integrating by parts where possible to eliminate the derivatives of the variations. The results of this straightforward procedure are

in U direction:

$$-N_{\xi,\xi} - (N_{\xi}U,_{\xi}),_{\xi} + \frac{1}{r^2}(N_{\theta}U,_{\theta}),_{\theta} - \frac{1}{r}N_{\xi\theta},_{\theta} - \frac{1}{r}\left[(N_{\xi\theta}U,_{\xi}),_{\theta} + (N_{\xi\theta}U,_{\theta}),_{\xi}\right] + \rho h\ddot{U} + pW,_{\xi} = 0 \tag{6a}$$

in V direction:

$$-(N_{\xi}V,_{\xi}),_{\xi} - \frac{1}{r}N_{\theta},_{\theta} - \frac{1}{r^2}\left[N_{\theta}(V,_{\theta} + W)\right],_{\theta} - \frac{1}{r^2}N_{\theta}(W,_{\theta} - V) - N_{\xi\theta},_{\xi} - \frac{1}{r}\left[N_{\xi\theta}(V,_{\theta} + W)\right],_{\xi} - \frac{1}{r}(N_{\xi\theta}V,_{\xi}),_{\theta} - \frac{N_{\xi\theta}}{r}W,_{\xi} + \rho h\ddot{V} - p\left(-\frac{1}{r}W,_{\theta} + \frac{V}{r}\right) = 0 \tag{6b}$$

in W direction:

$$-(N_{\xi}W,_{\xi}),_{\xi} + \frac{N_{\theta}}{r} + \frac{N_{\theta}}{r^2}(V,_{\theta} + W) - \frac{1}{r^2}\left[N_{\theta}(W,_{\theta} - V)\right],_{\theta} + \frac{1}{r}\left(N_{\xi\theta}V,_{\xi}\right) - \frac{1}{r}\left[N_{\xi\theta}W,_{\xi}\right],_{\theta} - \frac{1}{r}\left[N_{\xi\theta}(W,_{\theta} - V)\right],_{\xi} + \rho h\ddot{W} - p\left[U,_{\xi} + \frac{1}{r}V,_{\theta} + \frac{W}{r}\right] = 0 \tag{6c}$$

with the corresponding boundary conditions

$$\begin{aligned} N_{\xi} + N_{\xi}U,_{\xi} + \frac{1}{r}N_{\xi\theta}U,_{\theta} = 0 \quad &\text{or } U = 0 \\ N_{\xi}V,_{\xi} + N_{\theta\xi} + \frac{1}{r}N_{\theta\xi}(V,_{\theta} + W) = 0 \quad &\text{or } V = 0 \\ N_{\xi}W,_{\xi} + \frac{1}{r}N_{\xi\theta}(W,_{\theta} - V) = 0 \quad &\text{or } W = 0 \end{aligned} \tag{7}$$

The equations of motion (6) represent the sum of the forces along coordinates of the undeformed surface and are valid for large displacements, small strains, and moderately large rotations.

Vibration equations. In the derivation of the vibration equations, the stress resultants and displacements are separated into parts associated with an initial axisymmetric prestress and parts associated with infinitesimal time dependent perturbed displacements about the prestressed state. Thus, the stress resultants and displacements in the total stress state are given by

$$\begin{aligned} N_\xi &= \overline{N}_\xi + \tilde{N}_\xi \\ N_\theta &= \overline{N}_\theta + \tilde{N}_\theta \\ N_{\xi\theta} &= \overline{N}_{\xi\theta} + \tilde{N}_{\xi\theta} \\ U &= \overline{U} + \tilde{U} \\ V &= \overline{V} + \tilde{V} \\ W &= \overline{W} + \tilde{W} \end{aligned} \tag{8}$$

where the bars indicate the prestressed state and the (orders of magnitude smaller) tilde quantities refer to the perturbed state. It is assumed that no additional external loading is associated with the perturbed state. Substituting equations (8) into equations (6) and (7) and subtracting out the initial equilibrium state yields the linearized equations governing the free vibrations of a prestressed cylindrical shell as follows:

In U direction:

$$\tilde{N}_{\xi,\xi} + \frac{1}{r}\tilde{N}_{\xi\theta,\theta} + \bar{N}_{\xi}\tilde{U}_{,\xi\xi} + \frac{1}{r^2}\bar{N}_{\theta}\tilde{U}_{,\theta\theta} - \rho h\ddot{\tilde{U}} - p\tilde{W}_{,\xi} = 0 \tag{9a}$$

In V direction:

$$\frac{1}{r}\tilde{N}_{\theta,\theta} + \tilde{N}_{\xi\theta,\xi} + \bar{N}_{\xi}\tilde{V}_{,\xi\xi} + \frac{1}{r^2}\bar{N}_{\theta}(\tilde{V}_{,\theta\theta} + 2\tilde{W}_{,\theta} - \tilde{V}) - \rho h\ddot{\tilde{V}} + \frac{p}{r}(-\tilde{W}_{,\theta} + \tilde{V}) = 0 \tag{9b}$$

In W direction:

$$\bar{N}_{\xi}\tilde{W}_{,\xi\xi} - \frac{\tilde{N}_{\theta}}{r} - \frac{1}{r^2}\bar{N}_{\theta}(\tilde{W} + 2\tilde{V}_{,\theta} - \tilde{W}_{,\theta\theta}) - \rho h\ddot{\tilde{W}} + p(\tilde{U}_{,\xi} + \frac{1}{r}\tilde{V}_{,\theta} + \frac{1}{r}\tilde{W}) = 0 \tag{9c}$$

with boundary conditions

$$\begin{aligned} \tilde{N}_{\xi} + \bar{N}_{\xi}\tilde{U}_{,\xi} = 0 \qquad & \text{or } \tilde{u} = 0 \\ \bar{N}_{\xi}\tilde{V}_{,\xi} + \tilde{N}_{\xi\theta} = 0 \qquad & \text{or } \tilde{v} = 0 \\ \bar{N}_{\xi}\tilde{W}_{,\xi} = 0 \qquad & \text{or } \tilde{w} = 0 \end{aligned} \tag{10}$$

In obtaining equations (9) and (10), it was assumed that the prestress deformations could be neglected and that the stress resultants in the prestressed state were constant. (With these assumptions, equations (9) agree with those used by Leipens (I-3) for a toroidal shell.) For a cylindrical membrane under internal pressure, these assumptions are justified for a linear vibration analysis.

Prestress state. The prestress in the cylindrical membrane is assumed to be satisfactorily given by the membrane state of stress. Thus, consistent with the assumption that the prestress deformations can be neglected, the prestress stress

resultants are

$$\bar{N}_\theta = pr \qquad \bar{N}_\xi = pr/2 \qquad \bar{N}_{\xi\theta} = 0 \tag{11}$$

where r is the undeformed radius of the shell.

Constitutive relations. Consistent with previous assumptions, the relation between the linearized stress resultants and strain are

$$\begin{aligned}
\tilde{N}_\xi &= B\left[\tilde{U}_{,\xi} + \frac{\nu}{r}\left(\tilde{V}_{,\theta} + \tilde{W}\right)\right] \\
\tilde{N}_\theta &= B\left[\frac{1}{r}\left(\tilde{V}_{,\theta} + \tilde{W}\right) + \nu\tilde{U}_{,\xi}\right] \\
\tilde{N}_{\xi\theta} &= \frac{B}{2}(1-\nu)\left(\frac{1}{r}\tilde{U}_{,\theta} + \tilde{V}_{,\xi}\right)
\end{aligned} \tag{12}$$

Solutions for Cylinder Vibrations

In their present form, equations (9) and (10) are partial differential equations with three independent variables. However, for this analysis, the θ and time dependence is removed by assuming a separable type solution

$$\begin{aligned}
\tilde{U} &= u(x)\cos n\theta\, e^{i\omega t} \\
\tilde{W} &= w(x)\cos n\theta\, e^{i\omega t} \\
\tilde{N}_\xi &= n_\xi(x)\cos n\theta\, e^{i\omega t} \\
\tilde{N}_\theta &= n_\theta(x)\cos n\theta\, e^{i\omega t} \\
\tilde{V} &= v(x)\sin n\theta\, e^{i\omega t} \\
\tilde{N}_{\xi\theta} &= n_{\xi\theta}(x)\sin n\theta\, e^{i\omega t}
\end{aligned} \tag{13}$$

where $X = \xi/L$. Substituting equations (13) into equations (9) and (10) and making use of equations (12) yields the governing equations as follows:

$$\begin{aligned} F_{11}u'' + H_{11}u + G_{12}v' + G_{13}w' &= 0 \\ G_{21}u' + F_{22}v'' + H_{22}v + H_{23}w &= 0 \\ G_{31}u' + H_{32}v - F_{33}w'' + H_{33}w &= 0 \end{aligned} \tag{14}$$

with the corresponding boundary conditions

$$\begin{aligned} &\frac{1}{L}\left(1 + \frac{\overline{N}_\xi}{B}\right)u' + \frac{\nu}{r}(nv + w) = 0 && \text{or } u = 0 \\ &\frac{1}{L}\left(1 + \frac{\overline{N}_\xi}{B(1-\nu)}\right)v' - \frac{nu}{r} = 0 && \text{or } v = 0 \\ &\overline{N}\, w' = 0 && \text{or } w = 0 \end{aligned} \tag{15}$$

In equations (14) and (15), primes denote differentiation with respect to the nondimensional coordinate X. Also

$$\begin{aligned} F_{11} &= \left(\frac{r}{L}\right)^2 \left(1 + \frac{\overline{N}_\xi}{B}\right) \\ F_{22} &= \left(\frac{r}{L}\right)^2 \left(\frac{1-\nu}{2} + \frac{\overline{N}_\xi}{B}\right) \\ F_{33} &= \left(\frac{r}{L}\right)^2 \frac{\overline{N}_\xi}{B} \\ H_{23} = H_{32} &= -n - 2n\frac{\overline{N}_\theta}{B} + \frac{npr}{B} \\ G_{12} = -G_{21} &= \frac{rn}{L}\left(\frac{1+\nu}{2}\right) \\ G_{13} = G_{31} &= \frac{r}{L}\left(\nu - \frac{pr}{B}\right) \end{aligned} \tag{16}$$

$$H_{11} = \frac{-n^2}{2}(1-\nu) - \frac{\bar{N}_\theta n^2}{B} + r^2\frac{\rho h\omega^2}{B}$$

$$H_{22} = -n^2 - \frac{\bar{N}_\theta}{B}(1+n^2) + \frac{pr}{B} + r^2\frac{\rho h\omega^2}{B}$$

$$H_{33} = -1 - \frac{\bar{N}_\theta}{B}(1+n^2) + \frac{pr}{B} + r^2\frac{\rho h\omega^2}{B}$$

For this investigation, it was originally intended to determine the natural frequencies of a cantilevered cylindrical membrane. However, equations (15) show that for this boundary condition the impossible condition of zero slope ($w' = 0$) is required at the free end. (Such a condition also appears in the problem of the "free end string" and can only be avoided by considerations of the bending stiffness of the structure.) Hence while results could be obtained for the cantilever boundary conditions, it is felt that more realistic and meaningful information can be presented by determining the natural frequencies for simply supported cylindrical membranes.

Numerical results for simply supported pressurized cylindrical membrane. The solutions of equations (14) which satisfy the $u = v = w = 0$ simple support boundary conditions are

$$u(x) = \alpha \sin m\pi x$$

$$v(x) = \beta \cos m\pi x \qquad (17)$$

$$w(x) = \gamma \sin m\pi x$$

Substituting equations (17) into equations (14) and requiring that the determinant of the coefficients α, β, and γ vanish, leads to the following sixth order characteristic equation for the determination of the natural frequencies.

$$-A\,\pi^6 m^6 + B\pi^4 m^4 - C\pi^2 m^2 + D = 0 \tag{18}$$

where

$$A = -F_{11}\,F_{22}\,F_{23}$$

$$B = -F_{22}\,G_{13}^2 - F_{33}(F_{11}H_{22} + H_{11}F_{22} - G_{12}^2) + H_{33}F_{11}F_{22}$$

$$C = -G_{13}^2\,H_{22} + G_{12}G_{13}H_{23} + G_{12}G_{13}H_{32} - F_{11}H_{23}^2 + H_{33} \times \tag{19}$$

$$(F_{11}\,H_{22} + H_{11}\,F_{22} - G_{12}^2) - H_{11}\,H_{22}\,F_{33}$$

$$D = H_{11}\,H_{22}\,H_{33} - H_{11}\,H_{23}^2$$

Equation (18) has been solved for the frequency parameter for a typical pressurized cylindrical membrane with R/L = .333, R/t = 500, 1000, and m = 1, 2 for various values of pr/Et from 0 to .002. This upper limit was chosen since it represents the maximum elastic strains for many engineering materials.

The effect on the natural frequency due to the internal pressure is illustrated in Figures I-1,2,3, and 4. The results indicate that for any given R/L, the effect of pressure on the natural frequency is approximately the same, if R/t is sufficiently small such that the shell approaches a true membrane. It is

also interesting to note that for no internal pressure, the frequency parameter of the membrane decreases monotonically to zero for an increase in circumferential wave number n. Since the frequency varies with the effective "stiffness" of the membrane, this is equivalent to a monotonic decrease in stiffness with an increase in n for no internal pressure. However, when internal pressure is added, it can be seen from the figures that the frequency, and hence the stiffness of the membrane is increased with an increase in n for n greater than 3 to 5.

These results have been compared with an approximate formula derived in reference (I-4) by using Donnell's theory and neglecting the inplane inertias. For large values of n, where Donnell's theory is applicable, the results were in good agreement.

Finally, calculations were also made using the results of this analysis but neglecting the inplane inertias. For the typical cases treated, the error introduced in neglecting the inplane inertia was of the order of five percent or less. Hence, for most practical cases it seems reasonable that this effect can be neglected.

References for Chapter I

I-1. Koiter, W. T.: A Consistent First Approximation in the General Theory of Thin Shells. The Theory of Thin Elastic Shells, W. T. Koiter, ed., Interscience Publ., Inc., 1960, pp. 12-33.

I-2. Langhaar, H. L.: Energy Methods in Applied Mechanics. John Wiley & Sons, Inc., 1962.

I-3. Liepins, Atis A. : Free Vibrations of the Prestressed Toroidal Membrane. AIAA J., vol. 3, No. 10, Oct. 1965, pp. 1924-1933.

I-4. Cooper, Paul A.: Effect of Shallow Meridional Curvature on the Vibration of Nearly Cylindrical Shells, NASA TN D-5143. April, 1969.

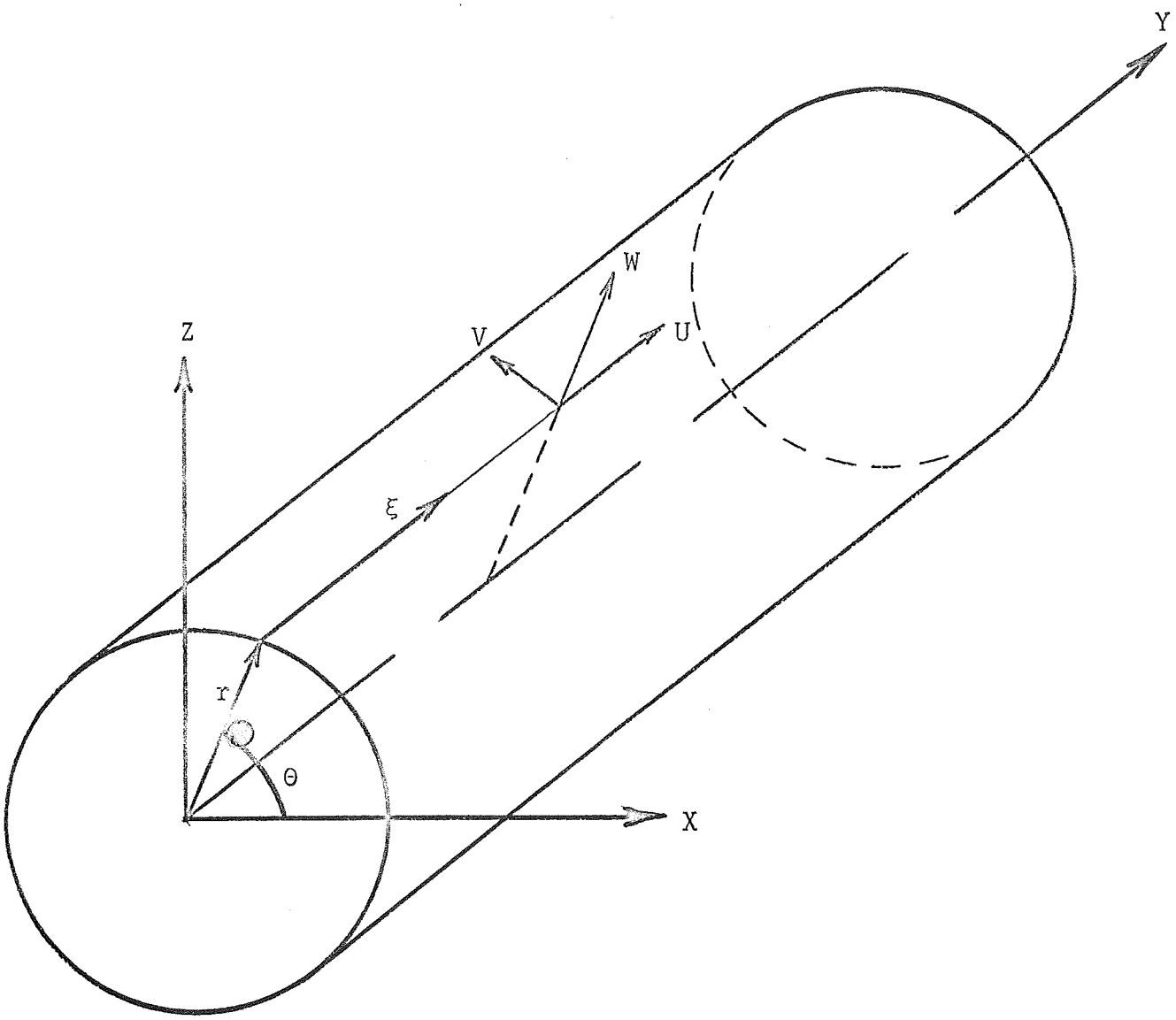

Figure I-1. Geometry of cylindrical membrane.

Figure I-1. Frequency Variation with Pressure

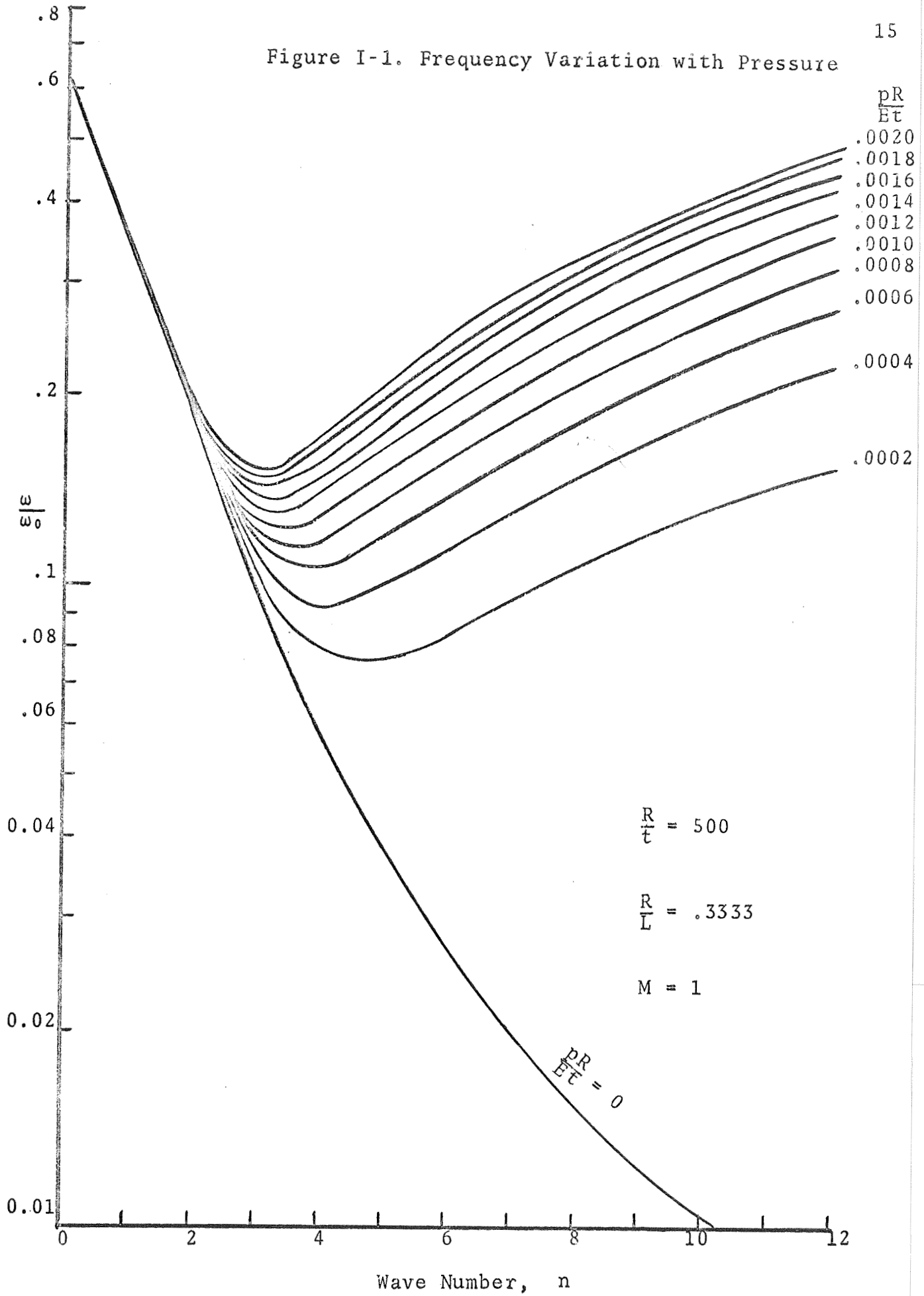

Figure I-2. Frequency Variation with Pressure

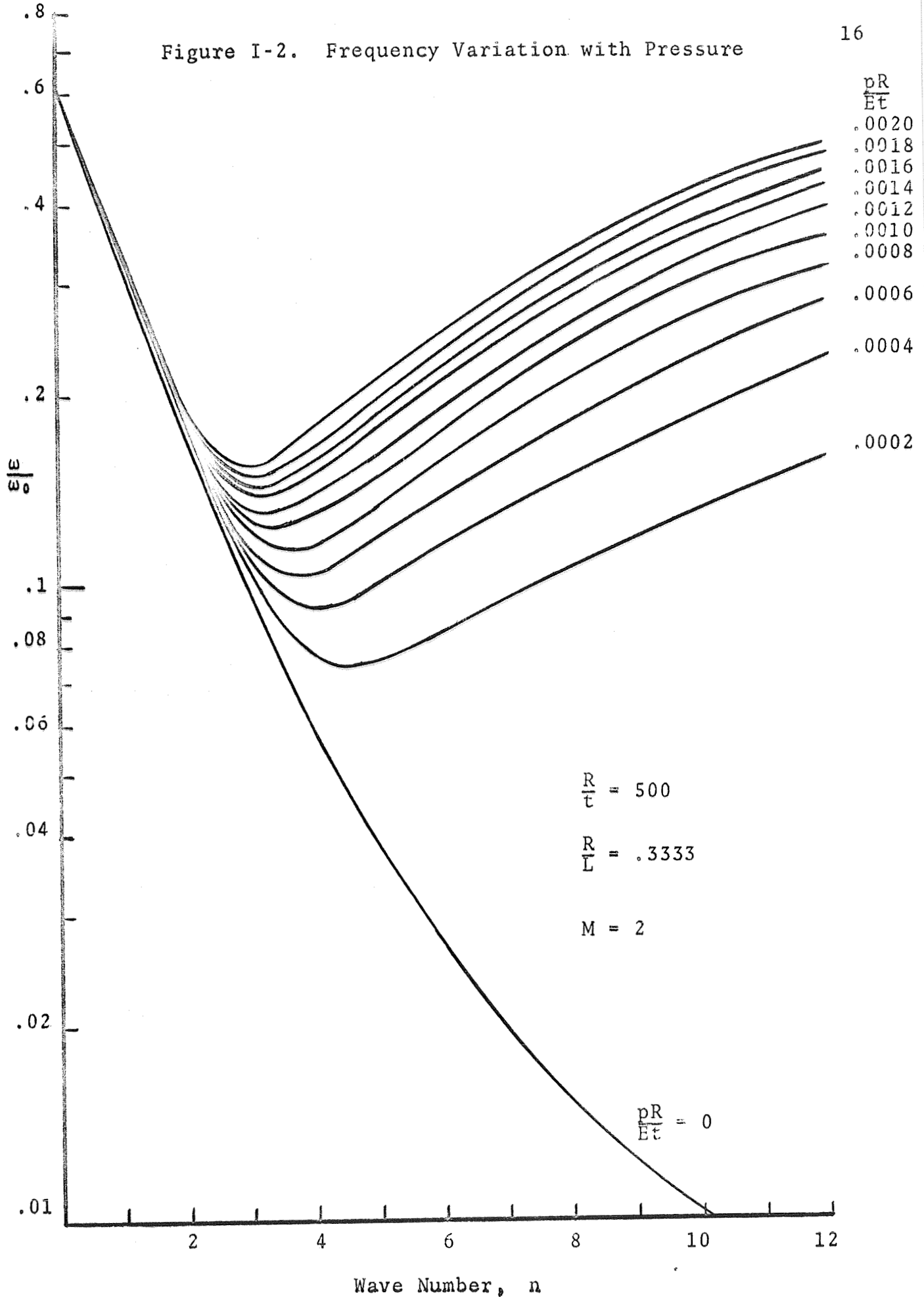

Figure I-3. Frequency Variation with Pressure

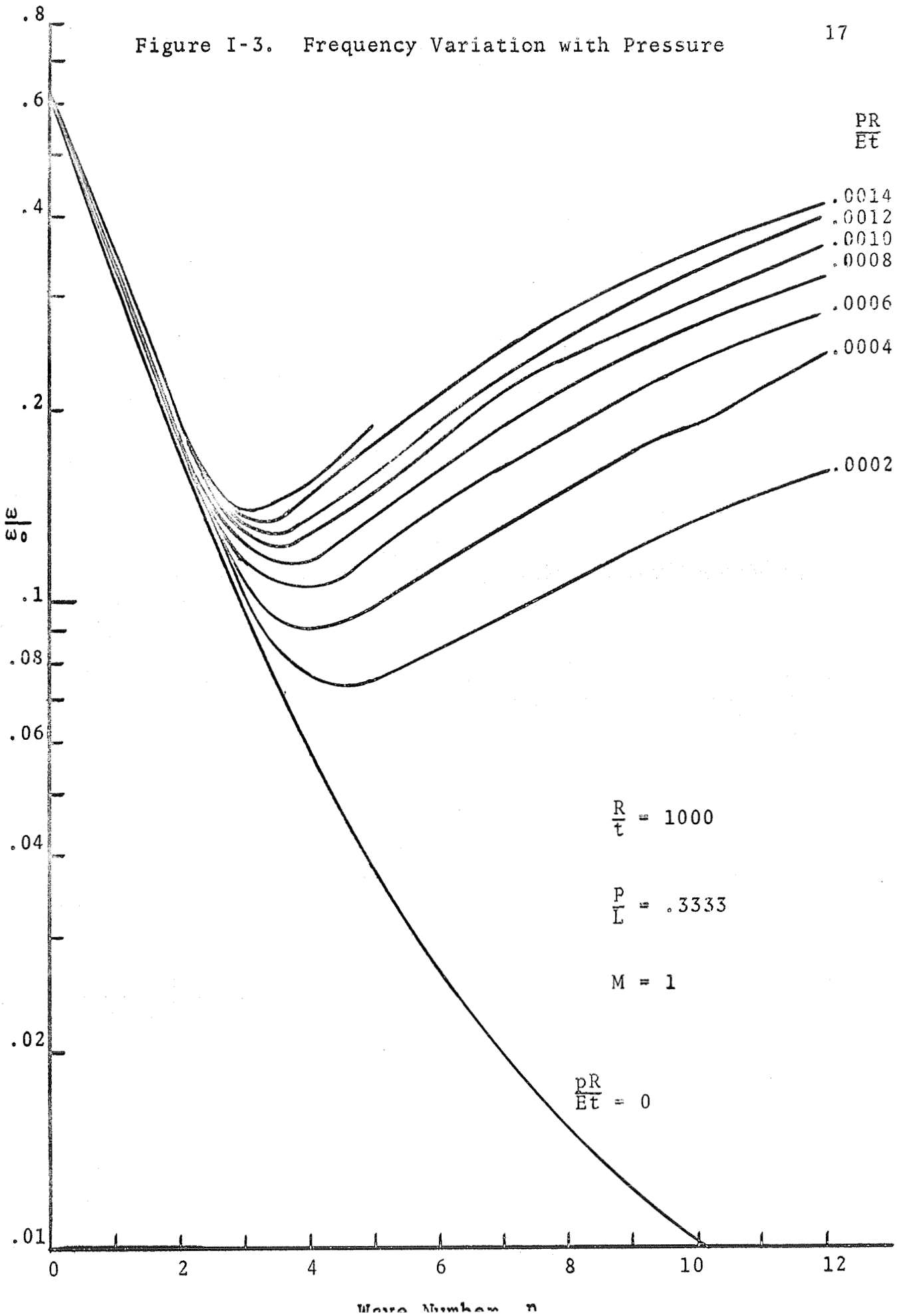

Figure I-4. Frequency Variation with Pressure

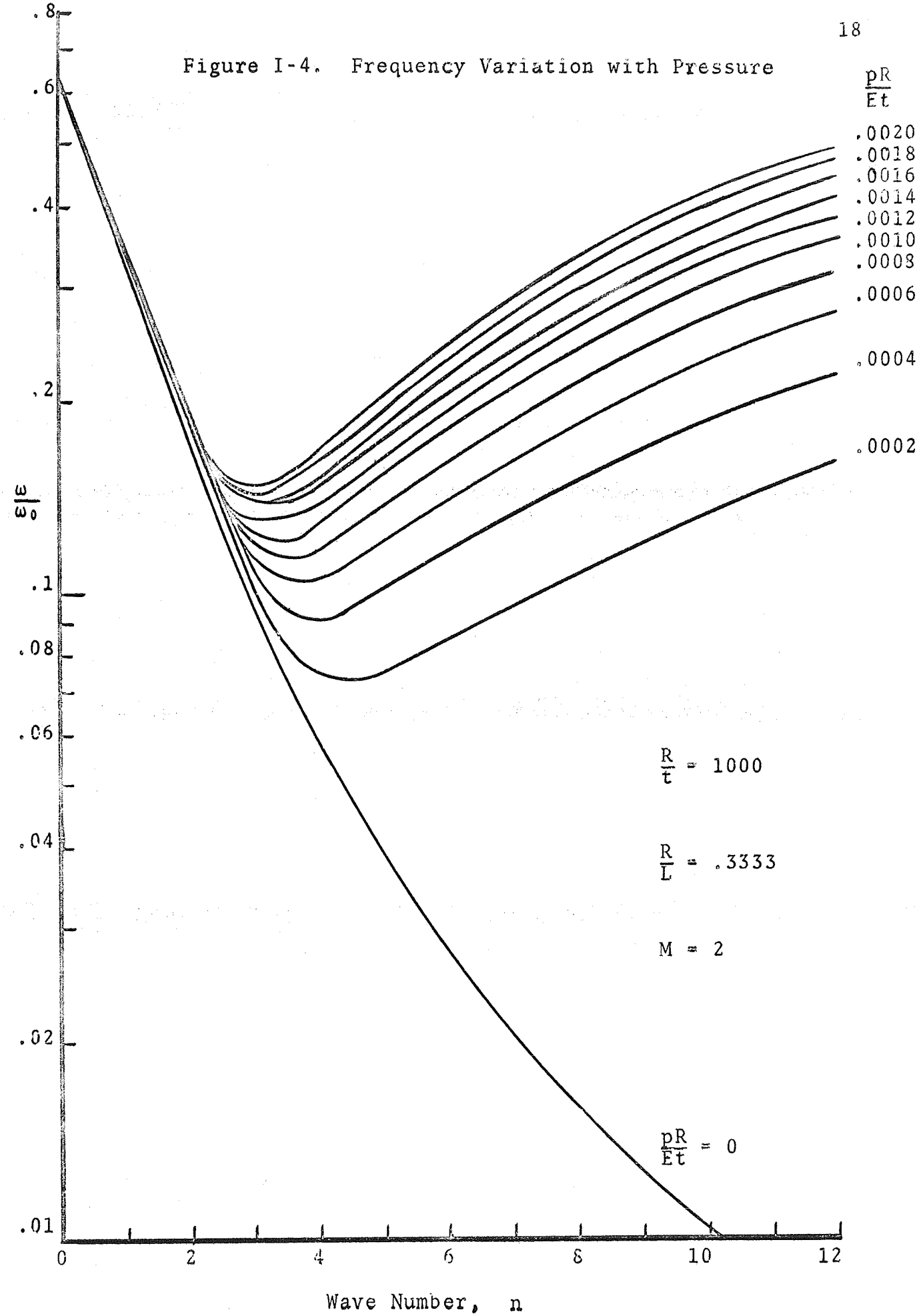

CHAPTER II

VIBRATIONS OF INFLATED CYLINDRICAL BEAMS

Summary

A linearized set of governing equations is developed for the vibratory motion of inflated cylindrical beams. Natural frequencies are calculated for the first five normal modes of a cantilevered beam. The frequency values are given as a function of an effective shear stiffness parameter. The results are applicable to orthotropic materials for the beam walls. The method of analysis yields frequency values for the reduced case of no internal pressure and infinite transverse shear stiffness which compare favorably to classical frequency values.

II-A Introduction

The objective in this chapter is to derive and solve the equations governing the vibratory behavior of inflated cylindrical beams. The analysis is based on a procedure similar to that developed in detail in References (II-1) and (II-2) for the buckling of inflated beams and rings of circular cross section. Hamilton's principle is used to derive the governing equations. The effects of internal pressure and transverse shear deformations are accounted for by referring the local displacements in the beam wall to rigid body translations and cross sectional rotations. The results are valid for moderately large deflections and rotations of the beam.

The results are presented in a graphical form showing frequency values as a function of the internal pressure and transverse shear stiffness. The effect of internal pressurization is shown to depend on the inclusion of the transverse shear stiffness of the beam in the analysis. A comparison with known solutions for the case of no internal pressure and infinite shear stiffness provides an indication of the validity of the results found in this investigation.

II-B Analysis

A segment of the pressurized cylindrical beam configuration and the coordinate systems are shown in Figure II-1. The displacements u, v, w of points on the surface are related to rigid body translations and rotations about the centroidal axis of the beam. Translations u_i and rigid body rotations ω_i of the centroidal axis are referred to a local cartesian coordinate system with its origin along the centroidal axis.

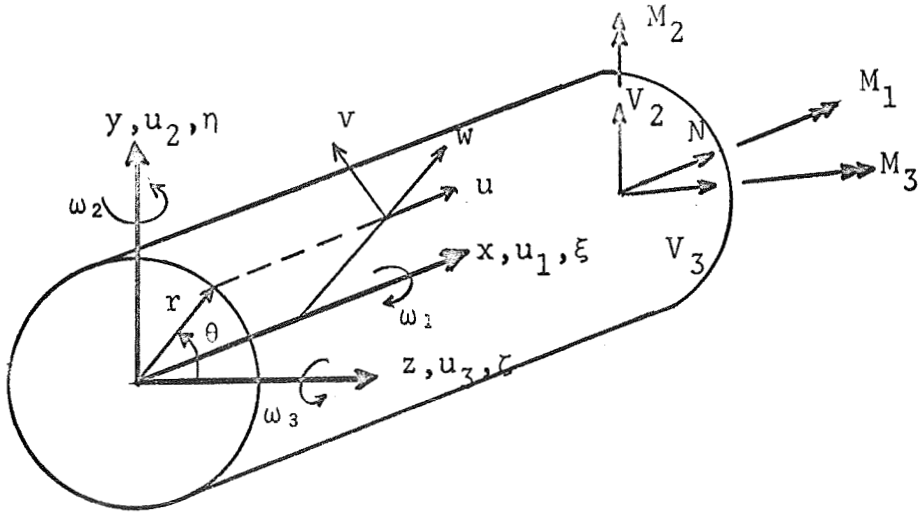

Figure II-1 Coordinates, displacements, and load resultants on inflatable cylindrical beam.

Certain simplifying assumptions have been made in this analysis: (1) The beam is considered to be a membrane in that the local bending stiffness of the walls is neglected, (2) the beam vibrates without localized wrinkling of the membrane walls, (3) any cross section of the beam remains rigid in its own plane so that the cross section remains circular and the resulting deformations can be characterized by the six rigid-body motions of translation and rotation of the cross section, (4) the rigid body rotations are small enough for the displacements on the surface of the beam to be represented by the vector sums of the displacements due to translation and rotations of a cross section.

Derivation of Governing Equations

The equations governing the vibration behavior of a prestressed cylindrical beam are obtained from the variational form of Hamilton's principle

$$\delta \int_{t_1}^{t_2} (\pi_1 + \pi_2 - T)\, dt = 0 \qquad (1)$$

where π_1 is the change in strain energy, π_2 is the potential energy change of the internal pressure due to deformation and T is the change in kinetic energy of the beam.

Strain energy of the beam. Consistent with assumption (3), the strain ε_θ in the θ direction is neglected so that the strain energy π_1 for the beam becomes

$$\pi_1 = \tfrac{1}{2} \int_0^L \int_0^{2\pi} (N_x \varepsilon_x + N_{x\theta} \varepsilon_{x\theta})\, r\, d\theta\, dx \qquad (2)$$

where, for the cylinder, the pertinent nonlinear strain displacement relations are

$$\varepsilon_x = \frac{\partial u}{\partial x} + \tfrac{1}{2}\left[\left(\frac{\partial v}{\partial x}\right)^2 + \left(\frac{\partial w}{\partial x}\right)^2\right]$$

$$\varepsilon_x = \frac{\partial v}{\partial x} + \frac{1}{r}\frac{\partial u}{\partial \theta} + \frac{1}{r}\frac{\partial w}{\partial x}\left(\frac{\partial w}{\partial \theta} - v\right) \tag{3}$$

An immediate consequence of assuming zero circumferential strain is that the material constants E and G may be defined independently. Hence the results of this analysis will also be valid for orthotropic materials. In terms of translations and small rotations of a cross section, the local displacements u, v, w are given by (see ref. 1)

$$u = u_1 + r\omega_2\cos\theta - r\omega_3\sin\theta$$

$$v = u_2\cos\theta - u_3\sin\theta - r\omega_1 + \frac{r}{4}(\omega_2^2 - \omega_3^2)\sin 2\theta \tag{4}$$

$$w = u_2\sin\theta + u_3\cos\theta - \frac{r}{2}(\omega_1^2 + \omega_2^2\cos^2\theta + \omega_3^2\sin^2\theta)$$

so that the strain energy π_1 can be expressed in terms of the rotations and translations of a cross section as

$$\pi_1 = \tfrac{1}{2}\int_0^L (N\varepsilon_1 + M_2\kappa_2 + M_3\kappa_3 + M_1\gamma_1 + V_2\gamma_2 + V_3\gamma_3)\,dx \tag{5}$$

where

$$N_x = \frac{N}{2\pi r} + \frac{M_2}{\pi r^2}\cos\theta - \frac{M_3}{\pi r^2}\sin\theta$$

$$N_{x\theta} = -\frac{M_1}{2\pi r^2} + \frac{V_2}{\pi r}\cos\theta - \frac{V_3}{\pi r}\sin\theta$$

$$N = 2E\pi rh\epsilon_1 \qquad M_1 = 2G\pi r^3 h\gamma_1$$

$$V_2 = G\pi rh\gamma_2 \qquad M_2 = E\pi r^3 h\kappa_2 \tag{6}$$

$$V_3 = G\pi rh\gamma_3 \qquad M_3 = E\pi r^3 h\kappa_3$$

and

$$\epsilon_1 = u_1' + \tfrac{1}{2}\left(r^2\omega_1'^2 + u_2'^2 + u_3'^2\right)$$

$$\kappa_2 = \omega_2' - \omega_1' u_2'$$

$$\kappa_3 = \omega_3' - \omega_1' u_3' \tag{7}$$

$$\gamma_1 = \omega_1'$$

$$\gamma_2 = u_2' - \omega_3 + \omega_1 u_3'$$

$$\gamma_3 = u_3' + \omega_2 - \omega_1 u_2'$$

Primes denote differentiation with respect to x.

Potential energy of the pressurizing gas: The change in potential of the pressurizing gas,

$$\pi_2 = - p\Delta V \tag{8}$$

where p is the internal pressure and ΔV is the change in enclosed volume due to deformation, can be written in terms of u_i and ω_i as (see for instance ref.1,2)

$$\pi_2 = - p\pi r^2 \int_o^L \left[u_1' + u_2'\omega_3 - u_3'\omega_2 - \tfrac{1}{2}(\omega_2^2 + \omega_3^2) \right] dx \tag{9}$$

Kinetic energy of the beam. The kinetic energy for the beam is developed on the assumption that the kinetic energy of the gas is negligible in comparison with the mass of the beam.

Then

$$T = \pi\rho h \int_o^L \left[\dot{u}_1^2 + \dot{u}_2^2 + \dot{u}_3^2 + \frac{r^2}{2}(\dot{\omega}_2^2 + \dot{\omega}_3^2 + 2r^2\dot{\omega}_1^2) \right] dx \tag{10}$$

where ρ = mass density of the fabric walls of the beam.

The nonlinear equations governing the behavior of the beam are now obtained by substituting equations (5), (9), and (10) into (1), and utilizing the fundamental lemma of the calculus of variations. Performing this operation and neglecting the twist about the longitudinal axis (which is usually small) the nonlinear equations become

$$N' = c\ddot{u}_1$$

$$(Nu_2')' + V_2' - P\omega_3' = c\ddot{u}_2$$

$$(Nu_3')' + V_3' + P\omega_2' = c\ddot{u}_3$$

$$M_2' - V_3 - P\,(u_3' + \omega_2) = k\ddot{\omega}_2 \qquad (11)$$

$$M_3' + V_2 + P\,(u_2' - \omega_3) = k\ddot{\omega}_3$$

where

$$c = 2\pi\rho h \qquad k = \pi\rho h r^2 \qquad P = p\pi r^2 \qquad (12)$$

The corresponding boundary conditions are, at x = 0 and L

$$u_1 = 0 \quad \text{or} \quad N - P = 0$$

$$u_2 = 0 \quad \text{or} \quad Nu_2' + V_2 - P\omega_3 = 0$$

$$u_3 = 0 \quad \text{or} \quad Nu_3' + V_3 + P\omega_2 = 0 \qquad (13)$$

$$\omega_2 = 0 \quad \text{or} \quad M_2 = 0$$

$$\omega_3 = 0 \quad \text{or} \quad M_3 = 0$$

Equations (6) and (11) constitute a system of 10 equations and 10 unknowns.

Solutions of Vibration Equations

Equations (11) are now used to obtain solutions for the vibration characteristics of an inflatable cylindrical beam with one end fixed and the other end free. In order that this be accomplished equations (11) are perturbed in the usual manner and the terms due to prestress are retained. The corresponding terms due to prestress deformations are neglected. Then the "linear" equations governing the free vibration behavior of an inflated beam become

$$2E\pi rh\, u_1'' = c\ddot{u}_1 \tag{14a}$$

$$P(u_2'' - \omega_3') + G\pi rh(u_2'' + \omega_2') = c\ddot{u}_2 \tag{14b}$$

$$P(u_3'' + \omega_2') + G\pi rh(u_3'' + \omega_2') = c\ddot{u}_3 \tag{14c}$$

$$E\pi r^3 h\omega_2'' - G\pi rh(u_3' + \omega_2) - P(u_3' + \omega_2) = k\ddot{\omega}_2 \tag{14d}$$

$$E\pi r^3 h\omega_3'' + G\pi rh(u_2' - \omega_3) + P(u_2' - \omega_3) = k\ddot{\omega}_3 \tag{14e}$$

with the corresponding boundary conditions at $x = 0$

$$u_1 = 0 \qquad \omega_3 = 0$$

$$u_3 = 0 \qquad u_2 = 0$$

$$\omega_2 = 0 \tag{15}$$

at $x = L$

$$u_1' = 0 \qquad \omega_3' = 0$$

$$u_3' + \omega_2 = 0 \qquad u_2' - \omega_3 = 0 \tag{15}$$

$$\omega_2' = 0$$

Equations (14) correspond to the Timoshenko beam equations (ref. 3) with the additional effects of internal pressure and large lateral displacements accounted for.

It will be noted from equations (14b, 14e) and equations (14c, 14d) that the inplane rotation and displacement, ω_3 and u_2 respectively, are uncoupled from the out-of-plane rotation and displacement, ω_2 and u_3 respectively. This is a consequence of neglecting twist about the longitudinal axis and of the beam cross section being axisymmetrical. In addition, the term involving the axial displacement u_1 appears in only one uncoupled equation, the solution of which is the classical extensional vibration results of beams. Thus the extensional stiffness EA of the beam is uncoupled from the effects of bending and internal pressure.

An added simplification results when it is noted that the structure of equations (14b,e) are identical to equations (14c,d) so that for this analysis it is only necessary to solve one of these two sets of equations. The set of equations chosen for solution are equations (14b,e). These equations are

first uncoupled by differentiating (14b) with respect to x, solve for ω_3'', substitute into (14d) and solve for ω_3, then substitute this result into (14b). The results of this straight forward procedure are

$$\bar{a}\, u_2^{IV} + \bar{b}\, u_2'' + \bar{c}\, u_2 = 0 \tag{16}$$

where

$$a = \frac{1}{1 + \left(\frac{\omega}{\omega_0}\right)^2 \frac{1}{2} \left(\frac{r}{L}\right)^2 \Big/ \left(\bar{P} + \bar{K}\right)} \qquad b = -\left(\frac{\omega}{\omega_0}\right)^2 \frac{\left[\frac{1}{2}\left(\frac{r}{L}\right)^2 + \frac{1}{\bar{P} + \bar{K}}\right]}{1 + \left(\frac{\omega}{\omega_0}\right)^2 \frac{1}{2} \left(\frac{r}{L}\right)^2 \Big/ \left(\bar{P} + \bar{K}\right)} \tag{17}$$

$$\bar{c} = \left(\frac{\omega}{\omega_0}\right)^2 \qquad \left(\frac{\omega}{\omega_0}\right)^2 = \frac{\omega^2}{(EI/cL^4)} \qquad \bar{P} = \frac{PL^2}{EI} \qquad \bar{K} = G\pi rh\frac{L^2}{EI}$$

and primes denote $\partial/\partial\xi$, $\xi = x/L$.

With the solution for u_2 known, the expression for ω_3 can be obtained as

$$\omega_3 = \frac{1}{L}\left(\bar{d}\, u_2' + \bar{e}\, u_2''\right) \tag{18}$$

where

$$\bar{d} = \frac{1}{\bar{a}}\left[1 - \frac{(\omega/\omega_0)^2}{(\bar{P} + \bar{K})^2}\right] \qquad \bar{e} = \frac{1}{a}\left(\frac{1}{\bar{P} + \bar{K}}\right) \tag{19}$$

The solution of equation (16) is

$$u_2 = a_1 e^{s_1 x} + a_2 e^{s_2 x} + a_3 e^{s_3 x} + a_4 e^{s_4 x} \tag{20}$$

and the corresponding solution to equation (18) is

$$\omega_3 L = a_1 q_1 e^{s_1 x} - a_2 q_1 e^{-s_1 x} + a_3 q_3 e^{s_3 x} - a_4 q_3 e^{-s_3 x} \tag{21}$$

where

$$s_1 = -s_2 = \sqrt{x_1} \qquad s_3 = -s_4 = \sqrt{x_2}$$

$$2x_{1,2} = -\frac{\bar{b}}{\bar{a}} \pm \sqrt{\left(\frac{\bar{b}}{\bar{a}}\right)^2 - 4\left(\frac{\bar{c}}{\bar{a}}\right)} \tag{22}$$

$$q_1 = s_1 (\bar{d} + \bar{e}\, s_1^2)$$

$$q_3 = s_3 (\bar{d} + \bar{e}\, s_3^2)$$

The boundary conditions are

$$\begin{aligned} u_2 &= 0 \quad \text{at} \quad \xi = 0 \\ \omega_3 &= 0 \quad \text{at} \quad \xi = 0 \\ \omega_3' &= 0 \quad \text{at} \quad \xi = 1 \\ u_2' - L\omega_3 &= 0 \quad \text{at} \quad \xi = 1 \end{aligned} \tag{23}$$

Applying these boundary conditions to equations (20) and (21) yields the following determinant of the coefficients a_i which must be zero for a nontrivial solution.

$$\begin{bmatrix} 1 & 1 & 1 & 1 \\ q_1 & -q_1 & q_3 & -q_3 \\ q_1 s_1 e^{s_1} & q_1 s_1 e^{-s_1} & q_3 s_3 e^{s_3} & q_3 s_3 e^{-s_3} \\ (s_1 - q_1)e^{s_1} & (-s_1 + q_1)e^{-s_1} & (s_3 - q_3)e^{s_3} & (-s_3 + q_3)e^{-s_3} \end{bmatrix} = 0 \quad (24)$$

Discussion of Results

The roots $(\omega/\omega_0)^2$ of the determinant (eqn. 24) yields the natural frequencies for an inflatable cantilever cylindrical beam once the shear stiffness parameter $1/(\overline{P} + \overline{K})$ and the length to radius ratio r/L, have been specified. Such calculations have been made for various configurations and the results plotted in Figure II-1. In Figure II-1, the nondimensional frequency parameter $-(\omega/\omega_0)^2$ has been plotted against the nondimensional shear stiffness parameter $1/(\overline{P} + \overline{K})$ for the first five modes of vibration. It was found that the influence of beam depth was negligible for $L/r \geq 20$ and accordingly the results shown in the figure are applicable for typical beam dimensions $r/L \geq 20$.

Note in all cases that the frequency parameter decreases with an increase in the shear stiffness parameter $1/(\overline{P} + \overline{K})$. This decrease is especially notable for small values of $1/(\overline{P} + \overline{K})$.

In this regard, it is pointed out that the values of $(\omega/\omega_0)^2$ for $1/(\overline{P} + \overline{K}) = 0$ cannot be obtained from equation (24), since if from equation (18) $1/(\overline{P} + \overline{K}) = 0$ then $\omega_3 L = u_2'$ which corresponds to the last of the boundary conditions (eqn. 23). Hence, since the equation of motion is the same as the boundary conditions for all x, then the last line of the determinant (eqn. 24) is identically zero and the determinant thus has no nontrivial solution. However, values of $(\omega/\omega_0)^2$ corresponding to $1/(\overline{P} + \overline{K}) = 0$ can be obtained from classical beam theory (see ref. 3, for example) and the dotted lines in Figure 1 represent extrapolation from these classical values to the first calculated values of $(\omega/\omega_0)^2$ for $1/(\overline{P} + \overline{K}) = 0.02$.

Concluding Remarks

A theoretical investigation of the vibration characteristics of a pressurized cylindrical cantilever beam has been carried out with finite shear stiffness and appropriate contributions from the internal pressure taken into account. The equations governing the natural frequencies have been derived and solved, and the results plotted in a usable format.

The major results of this investigation are: 1. Shear stiffness of the beam wall material and internal pressure both contribute to the effective transverse shear stiffness of the beam, which in turn strongly influences vibration characteristics. 2. The effect of radius to length ratio of the beam on the natural frequencies are negligible for typical beam dimensions of say $L/r \geq 20$.

References

1. Fichter, W. B.: A Theory of Inflated Thin-Wall Cylindrical Beams. NASA TN D-3466, 1966.

2. Weeks, G. E.: Buckling of A Pressurized Toroidal Ring Under Uniform External Loading.

3. Thomson, W. T.: Vibration Theory and Applications, Prentice Hall, Inc., Englewood Cliffs, N. J., 1965.

Figure II-1. Natural Frequencies of Cantilever Inflatable Beam For $L/r \geq 20$

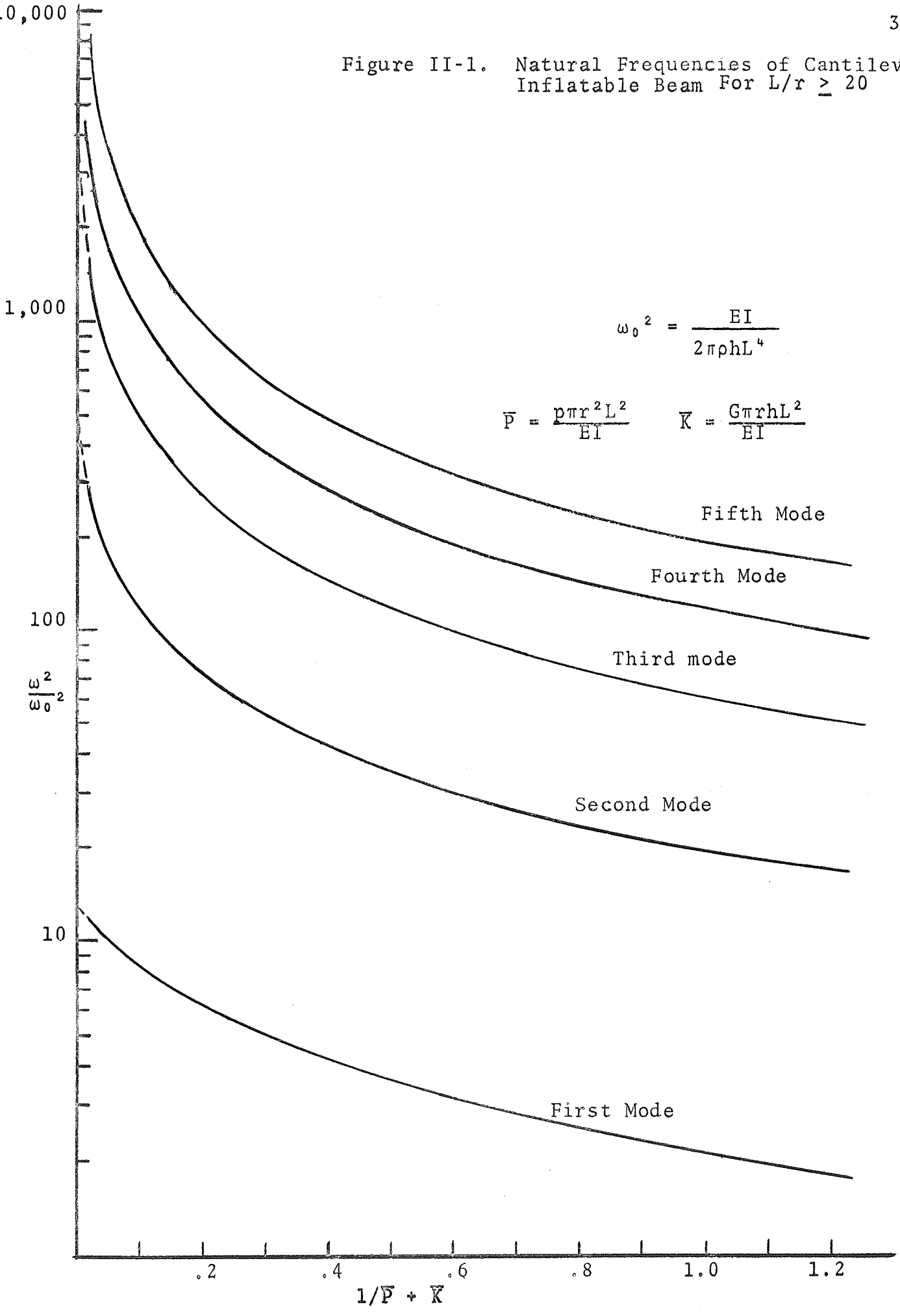

CHAPTER III

DYNAMIC RESPONSE OF RODS SUBJECTED TO GYROSCOPIC MOTION

Summary

Nonlinear equilibrium equations are derived and solved numerically for a flexible cantilever rod inclined to, and rotated about the vertical at a constant angular velocity. Solutions are obtained using both the Runge-Kutta integration procedure and the Taylor series expansion. Results are presented in the form of initial and terminal values of the dependent variables as functions of a nondimensional angular velocity parameter. The results of this analysis are also applicable for slender pressurized tubes.

III-A Introduction

This chapter is concerned with the derivation and solution of the nonlinear differential equations governing the motion of a flexible cantilever rod inclined to, and rotated about the vertical at a constant angular velocity. In the derivation of the equations, it is assumed that plane sections remain plane, shear deformation can be neglected, and the rod is inextensible. Numerical solutions are obtained using a fixed step Runge-Kutta integration procedure and a Taylor series expansion. The results of the analysis are applicable to the case of a pressurized tube with appropriate definitions of the dependent variables.

In order to make the results of this analysis applicable to a wide class of slender rod configurations, nondimensional

values of bending moment, tension, and shear at the fixed end, and nondimensional values of axial and transverse deflection, slope, and centrifugal force, at the free end are plotted as functions of a nondimensional parameter which characterizes the angular velocity, mass, length, and bending stiffness of the rod. These results are presented for the case where the slender rod is rotated uniformly in a gravity free environment.

Finally, a check on the validity of the results of this theoretical analysis is made by comparing with results obtained from experiment. The agreement was excellent. A more detailed discussion of the comparison between theory and experiment are given in another section of this report.

III-B Analysis

Consider a thin extensible rod of length L, weight per unit length p, mass per unit length m, and bending stiffness EI, cantilevered at one end and inclined at an angle α with respect to vertical. If in addition to the weight p, the rod is rotated about the vertical at a constant angular velocity, the deformed configuration is as shown in Figure III - 1a. A point on the undeformed rod defined by the coordinates x and α is displaced axially (u) and transversely (w) to a point on the deformed arc located by the coordinate s and the slope (θ) which the tangent makes with the reference axis. At this point on the deformed rod, the centrifugal force is

$$F_c = m\omega^2(-(u-x)\sin\alpha + w\cos\alpha) \qquad (1)$$

A freebody diagram of the deformed rod at this point (s,θ) is shown in Figure III-1b. Summing forces in the tangential direction (parallel to the deformed arc) yields the equilibrium equation.

$$\frac{dT}{ds} + Q\frac{d\theta}{ds} = p\cos(\alpha+\theta) - F_c\sin(\alpha+\theta) \qquad (2)$$

In a similar manner, the sum of the forces normal to the deformed arc results in the equilibrium equation

$$-\frac{dQ}{ds} + T\frac{d\theta}{ds} = -p\sin(\alpha+\theta) - F_c\cos(\alpha+\theta) \qquad (3)$$

In order that the sum of the moments are zero at any point

$$Q = dM/ds \qquad (4)$$

Equations (2), (3), and (4) are the differential equations governing the deformation of a flexible rod. They are also applicable for a pressurized tube if (a) the tension T is redefined to be T-qA where q is the internal pressure and A is the cross sectional area of the tube, (b) shear deformation is neglected and (c) the cross section remains circular. Such assumptions are reasonable for long slender configurations.

In order to obtain a solution to equation (2), (3) and (4), it is convenient to first rewrite them as a set of first order differential equations. This is accomplished in the following manner. From Figure III-1a, it is seen that the axial displacement u can be written as

$$u(s) = - \int_0^s \cos\theta ds + x \qquad (5)$$

and similarly the transverse deflection w can be written as

$$w(s) = \int_0^s \sin\theta ds \qquad (6)$$

From the Euler-Bernoulli hypothesis that plane sections remain plane, the relation between the bending moment and curvature is

$$M = EI \frac{d\theta}{ds} \qquad (7)$$

Now substituting equation (7) into equations (2) and (3) and differentiating equations (5) and (6) with respect to s, the following set of first order, nonlinear coupled differential equations are obtained.

$$\frac{dM}{ds} = Q$$

$$\frac{dT}{ds} = -\frac{QM}{EI} - F_c \sin(\alpha + \theta) + p\cos(\alpha + \theta)$$

$$\frac{dQ}{ds} = \frac{TM}{EI} + F_c \cos(\alpha + \theta) + p\sin(\alpha + \theta)$$

$$\frac{dQ}{ds} = \frac{M}{EI} \qquad (8)$$

$$\frac{d\xi}{ds} = -\cos\theta$$

$$\frac{dw}{ds} = \sin\theta$$

where

$$\xi = u - x \qquad (9)$$

The corresponding boundary conditions for the cantilever are

$$\begin{aligned} &\text{at} \quad s = 0 \qquad && \theta = \xi = w = 0 \\ &\text{at} \quad s = L \qquad && M = T = Q = 0 \end{aligned} \qquad (10)$$

The equations (8) together with the boundary conditions (10) constitute a well defined initial value problem.

These equations are now solved using (1) a Taylor series expansion and (2) a direct numerical integration procedure.

Although the latter technique is more flexible and in general a more feasible and accurate approach to the solution, the Taylor series expansion provides more physical insight into the solution of the problem. For this reason, it is included in this analysis.

Taylor Series Solution

The nonlinear equations (8) define six unknown dependent variables M, T, Q, θ, ξ, and w. However, if the slope θ and centrifugal force F_c were known, then the displacements u and w could be determined by integrating the last two of equations (8) and the moment M could be determined by differentiation from the fourth of equation (8). Then with the displacements, slope, and centrifugal force known, the tension and shear could be determined from integration of the second and third of equations (8).

To determine the slope and the centrifugal force, it is convenient to expand them in a Taylor series about the free end as follows

$$\theta(\xi) = \theta(0) + \xi\,\theta'(0) + \frac{\xi^2}{2}\,\theta''(0) + \cdots\cdots \tag{11}$$

$$F_c(\xi) = F_c(0) + \xi F_c'(0) + \frac{\xi^2}{2} F_c''(0) + \cdots\cdots$$

where $\xi = L-s$. The terms $\theta(0)$ and $F_c(0)$ at the free end are unknown. In addition, the coefficients of ξ in each of the equations are also unknown but as will presently be shown,

they can be expressed as functions only of $\theta(0)$ and $F_c(0)$. Thus, after the coefficients $\theta(0)$ and $F_c(0)$ are defined all other terms in (11) are known and the result is two nonlinear algebraic equations in the two unknowns $\theta(0)$ and $F_c(0)$.

To obtain a solution, values of $\theta(0)$ and $F_c(0)$ are assumed and iteratively adjusted until equations (11), evaluated at $\xi = L$, are zero. This iterative adjustment of the assumed values is obtained using the Newton Raphson method for simultaneous equations (ref. III-1). For this analysis the Taylor series (eqns. 11), were expanded through the eleventh derivative and results obtained for θ and F_c were compared with those obtained by a more accurate numerical integration procedure presented in the next section. Results were in excellent agreement for the slope and deflections. However, sufficiently accurate values for the internal forces and moment could only be obtained for values of $\theta(0) \leq 80^0$. For values of $\theta(0)$ greater than 80^0, additional terms in the series (11) are needed.

The coefficients appearing in equations (11) are given in detail in the appendix to this chapter. However, it is shown here how one proceeds to calculate these coefficients as a function only of $\theta(0)$ and $F_c(0)$. From equations (8) and (10)

$$\theta'(0) = - M(0)/EI \quad = 0$$

$$\theta''(0) = -M'(0)/EI = Q(0)/EI = 0$$

$$\theta'''(0) = Q'(0)/EI = p\sin\beta - F_c(0)\cos\beta$$

$$\theta^{IV}(0) = Q''(0)/EI = - F_c'(0)\cos\beta$$

where $\beta = \alpha + \theta(0)$ and primes denote differentiation with respect to ξ. But from equation (1)

$$F_c'(0) = -K \sin \beta$$

where $K = m\omega^2$ such that $\theta^{IV}(0)$ is defined. Continuing in this manner, all coefficients in equations (11) through any order derivative can be defined in terms of $\theta(0)$, $F_c(0)$. However, for higher order derivatives than those presented, the algebraic manipulations required to obtain the coefficients becomes prodigious.

To utilize the Newton Raphson procedure in solving the simultaneous equations, the second derivatives of equations (11) with respect to $\theta(0)$ and $F_c(0)$ are needed. The calculation of these derivatives are obvious and as such are not presented here. In addition, other methods such as regula falsi can be used which do not require the additional calculation of the second derivatives.

Solution by Numerical Integration

A more general technique of solution of equations (8) is that of numerical integration. For this analysis, the numerical integration is performed using a standard fourth order fixed step Runge Kutta integration routine. While more elaborate integration schemes such as variable step Runge-Kutta or predictor-corrector techniques could be used, it was found that the accuracy provided by such schemes was not necessary.

Since only three boundary conditions are known at each end, it is necessary to assume three additional conditions before the numerical integration can be performed. For this analysis the integration proceeds from the cantilevered end where the slope and two deflections are zero. The nonspecified initial values, bending moment, tension, and shear are assumed, the integration is performed, and the terminal (boundary) conditions at the free end are calculated. The initial data is then iteratively adjusted so that the solution to the initial value problem satisfies the boundary conditions of zero moment, tension, and shear at the (terminal) free end.

For this analysis, the initial data is iteratively adjusted by solving the variational equations of the original differential equations in conjunction with Newtons method. This basic procedure is similar to that which has been briefly outlined in references (1) and (2) for one dependent variable. For completeness, the details of the procedure are now outlined for the general case of M differential equations with M dependent variables. The results are then applied to the particular set of equations (8) and (10).

Consider the set of coupled nonlinear first order differential equations defined by $Y_i' = f_i\ (x, Y_i)$, $i = 1,M$ with solutions $Y_i = Y_i\ (x, A_i)$ where the A_i ($A_i = Y(0)$) are the M initial conditions. If these M initial conditions were known, the equations could be solved by direct numerical integration. However, for the general nonlinear two point boundary value problem, K of these M initial conditions are unknown ($K < M$) so

that to obtain a solution by integration, K values must be assumed for the unknown initial conditions. If the integration proceeds from left to right the resulting solution will not in general satisfy the boundary conditions on the right end. Thus the K initial values must be corrected and the equations again solved until the K initial values result in correct boundary values at the terminal point. A systematic procedure for obtaining these iterates is as follows.

Form the following functions with the dependent variables that are unknown at x = 0 but which at x = b are known, i.e.

$$f_i = Y_i\,(b,A_1,A_2 \ldots A_K) - P_i \qquad i = 1,K \tag{12}$$

where the P_i are the known values of $Y_i (i = 1,K)$ at x = b. It is obvious that if the $A_1, \ldots A_K$ are the correct initial values then the functions defined by equations (12) are zero. Now approximate these f_i by the linear parts of their Taylor series in the neighborhood of $A_{i_{n-1}}$ where $A_{i_{n-1}}$ denotes the approximate initial values

$$f_i(b,A_1,A_2, \ldots A_K) = f_i(b,A_1, \ldots A_K)_{n-1} + (A_1 - A_{i_{n-1}})* \frac{\partial f_i}{\partial A_1}\Big|_{n-1} + (A_2 - A_{2_{n-1}}) \frac{\partial f_i}{\partial A_2}\Big|_{n-1} + \ldots (A_K - A_{K_{n-1}})* \frac{\partial f_i}{\partial A_K}\Big|_{n-1} \tag{13}$$

and i = 1, K. Since, by definition the left sides of equations (13) are zero at $A_i = A_{i_n}$ (where A_{i_n}, denotes the correct initial values), they can be rewritten in the form

$$\{A_j\}_n = \{A_j\}_{n-1} - \left[C_{jq}\right]^{-1}_{x=b} \{f_q(b, A_1, \ldots A_K)\}_{n-1} \qquad (14)$$

with j = 1, K and q = 1,M. The { } denote column matrices and the [ ] denote square matrices. The C matrix in equations (14), evaluated at x = b, is defined from equations (13) as

$$C_{iq} = \frac{\partial f_i}{\partial A_q} \qquad \begin{matrix} i = 1,K \\ q = 1,M \end{matrix} \qquad (15)$$

Thus if initial values $A_{i_{n-1}}$ are assumed so that the C and f matrix can be evaluated, equations (14) can be used to calculate a corrected or improved set of the initial values A_{i_n}. The problem now remains to determine the elements of the C matrix. For this analysis, these elements are determined by deriving and solving the variational equations of the original first order equations. The variational equations are derived as follows: Let $Y_i(x, A_1, \ldots A_K)$ denote solutions of $Y_i' = f_i(x, Y_i)$. Also, let $Z_{ij}(x, A_1, \ldots A_K)$ denote partial derivatives of $Y_i(x, A_1, \ldots A_K)$ relative to $A_1, A_2, \ldots A_K$, i.e.

$$Z_{ij} = \frac{\partial Y_i}{\partial A_j} \qquad \begin{matrix} i = 1,M \\ j = 1,K \end{matrix} \qquad (16)$$

From equations (16) the derivatives of Z_{ij} with respect to x are

$$Z'_{ij} = \frac{\partial Y'_i}{\partial Y_q} \frac{\partial Y_q}{\partial A_j} \qquad \begin{matrix} i = 1,M \\ j = 1,K \\ q = 1,M \end{matrix} \tag{17}$$

By making use of equations (16), equations (17) can be written in the compact form

$$Z'_{ij} = E_{iq} Z_{qj} \qquad \begin{matrix} i = 1,M \\ j = 1,K \\ q = 1,M \end{matrix} \tag{18}$$

Equations (18) are the variational equations of $Y_i(x, A_1, \ldots A_K)$ with the initial conditions

$$Z_{ij}(0, A_1, \ldots A_K) = \delta_{ij} \tag{19}$$

where δ_{ij} is the Kronecker delta. Now with solutions $Z_{ij}(x, A_i)$, the elements in the C matrix become just

$$C_{ij} = Z_{ij}(b, A_i) \tag{20}$$

Thus, with C_{ij} known, the right hand side of equations (14) can be evaluated so that the next set of initial values A_i can be calculated. This procedure is repeated until convergence

to correct initial values are obtained.

In summary, the step by step procedure for the solution of the nonlinear two point boundary value problem using the proposed algorithm is as follows:

1. Assume a set of initial values and solve the original set of nonlinear differential equations using any of the standard numerical integration schemes.
2. With these solutions known at a finite number of points in the interval $0 \leq x \leq b$, the elements in the E_{iq} matrix are defined at the same number of points. Now solve the K sets of differential equations (19) with initial values as per equation (20).
3. With these solutions known, the elements E_{ij} are defined such that the right hand side of equations (14) can be evaluated for the new set of initial values A_i.
4. Steps 1 through 3 are repeated until desired convergence to the correct initial values are obtained.

Application to equations (8) and (10). To apply the results of the previous section to the solution of equations (8) and (10), define the fundamental variables as follows:

$$\begin{aligned} Y(1) &= M \\ Y(2) &= T \\ Y(3) &= Q \\ Y(4) &= \theta \\ Y(5) &= \xi \\ Y(6) &= w \end{aligned} \qquad (21)$$

Then the differential equations (8) can be written

$$Y'(1) = Y(3)$$

$$Y'(2) = -\frac{Y(1)\ Y(3)}{EI} - F_c \sin(\alpha + Y(4)) + p \cos(\alpha + Y(4))$$

$$Y'(3) = \frac{Y(1)\ Y(2)}{EI} + F_c \cos(\alpha + Y(4)) + p \sin(\alpha + Y(4))$$

$$Y'(4) = Y(1)/EI \qquad (22)$$

$$Y'(5) = -\cos(Y(4))$$

$$Y'(6) = \sin(Y(4))$$

and $F_c = B\left[-Y(5)\sin\alpha + Y(6)\cos\alpha\right]$, $B = m\omega^2$ with boundary conditions

$$\begin{aligned} &\text{at } s = 0 && Y(4) = Y(5) = Y(6) = 0 \\ &\text{at } s = L && Y(1) = Y(2) = Y(3) = 0 \end{aligned} \qquad (23)$$

From equations (22), the nonzero coefficients of E_{iq} are

$$E_{11} = \frac{\partial Y'(1)}{\partial Y(3)} = 1.$$

$$E_{21} = \frac{\partial Y'(2)}{\partial Y(1)} = -Y(3)/EI$$

$$E_{23} = \frac{\partial Y'(2)}{\partial Y(3)} = -\frac{Y(1)}{EI} \qquad E_{24} = \frac{\partial Y'(2)}{\partial Y(4)} = F_c \cos(\alpha + Y(4)) - p \sin(\alpha + Y(4))$$

$$E_{25} = \frac{\partial Y'(2)}{\partial Y(5)} = B \sin\alpha \sin(\alpha + Y(4))$$

$$E_{26} = \frac{\partial Y'(2)}{\partial Y(6)} = -B \cos\alpha \sin(\alpha + Y(4))$$

$$E_{31} = \frac{\partial Y'(3)}{\partial Y(1)} = Y(2)/EI \qquad E_{32} = \frac{\partial Y'(3)}{\partial Y(2)} = Y(1)/EI$$

$$E_{34} = \frac{\partial Y'(3)}{\partial Y(4)} = -F_c \sin(\alpha + Y(4)) + p \cos(\alpha + Y(4))$$

$$E_{35} = \frac{\partial Y'(3)}{\partial Y(5)} = -B \sin\alpha \cos(\alpha + Y(4))$$

$$E_{36} = \frac{\partial Y'(3)}{\partial Y(6)} = B \cos\alpha \cos(\alpha + Y(4)) \qquad (24)$$

$$E_{41} = \frac{\partial Y'(4)}{\partial Y(1)} = 1/EI \qquad E_{54} = \frac{\partial Y'(5)}{\partial Y(4)} = \sin(Y(4))$$

$$E_{64} = \frac{\partial Y'(6)}{\partial Y(4)} = \cos(Y(4))$$

so that equations (18) become

(25)

$$\begin{bmatrix} Z'_{11} & Z'_{12} & Z'_{13} \\ Z'_{21} & Z'_{22} & Z'_{23} \\ Z'_{31} & Z'_{32} & Z'_{33} \\ Z'_{41} & Z'_{42} & Z'_{43} \\ Z'_{51} & Z'_{52} & Z'_{53} \\ Z'_{61} & Z'_{62} & Z'_{63} \end{bmatrix} = \begin{bmatrix} 0 & 0 & E_{13} & 0 & 0 & 0 \\ E_{21} & 0 & E_{23} & E_{24} & E_{25} & E_{26} \\ E_{31} & E_{32} & 0 & E_{34} & E_{35} & E_{36} \\ E_{41} & 0 & 0 & 0 & 0 & 0 \\ 0 & 0 & 0 & E_{54} & 0 & 0 \\ 0 & 0 & 0 & E_{64} & 0 & 0 \end{bmatrix} \begin{bmatrix} Z_{11} & Z_{12} & Z_{13} \\ Z_{21} & Z_{22} & Z_{23} \\ Z_{31} & Z_{32} & Z_{33} \\ Z_{41} & Z_{42} & Z_{43} \\ Z_{51} & Z_{52} & Z_{53} \\ Z_{61} & Z_{62} & Z_{63} \end{bmatrix}$$

Equations (22), (24), and (25) have been programmed on a digital computer and solutions obtained for various slender rod configurations. A discussion of the results obtained are presented in the next section.

Discussion of Results

Numerical results are presented in this section for the cantilever rod rotating about the vertical at a constant angular velocity in a gravity free (p = 0) environment. In Table III-1, nondimensional values of moment, tension, and shear at the fixed end are tabulated as functions of a nondimensional "frequency" parameter $mL^4\omega^2/EI$ for various values of α. With these calculated initial values, and with the known initial values of zero deflection, slope and centrifugal force at the fixed end, equations (22) can be integrated directly using any of the available integration subroutines. Also, for completeness, the values of slope, deflections, and centrifugal force at the free end are plotted in Figure III-2. As can be seen, for any given rod geometry, the deflections and slope become larger as the angular velocity is increased, the limiting values occurring as $\theta+\alpha$ approaches 90^0.

For low values of $mL^4\omega^2/EI$, the generalized forces at the fixed end and the generalized displacements at the free end are in good agreement with those obtained by linear theory. However, for values of $mL^4\omega^2/EI>5$, the results obtained between the linear and nonlinear theory begin to diverge. For the maximum values presented ($mL^4\omega^2/EI = 55.66$) the differences

between linear and nonlinear theory differ by as much as several hundred percent.

The validity of the numerical results presented here were substantiated by carefully controlled experiments. (The chapter on the experimental procedure and the results obtained is included in this report). The differences between the experimental values and those obtained numerically were usually no greater than five percent, even when the tip deflections were as much as 80 percent of the length of the rod.

References for Chapter III

III-1. Schied, F.: Numerical Analysis, (Schaums Outline Series), McGraw Hill Book Company, 1968.

III-2 Isaacson, E. and Keller, H. B.: Analysis of Numerical Methods. John Wiley & Sons, New York, 1966.

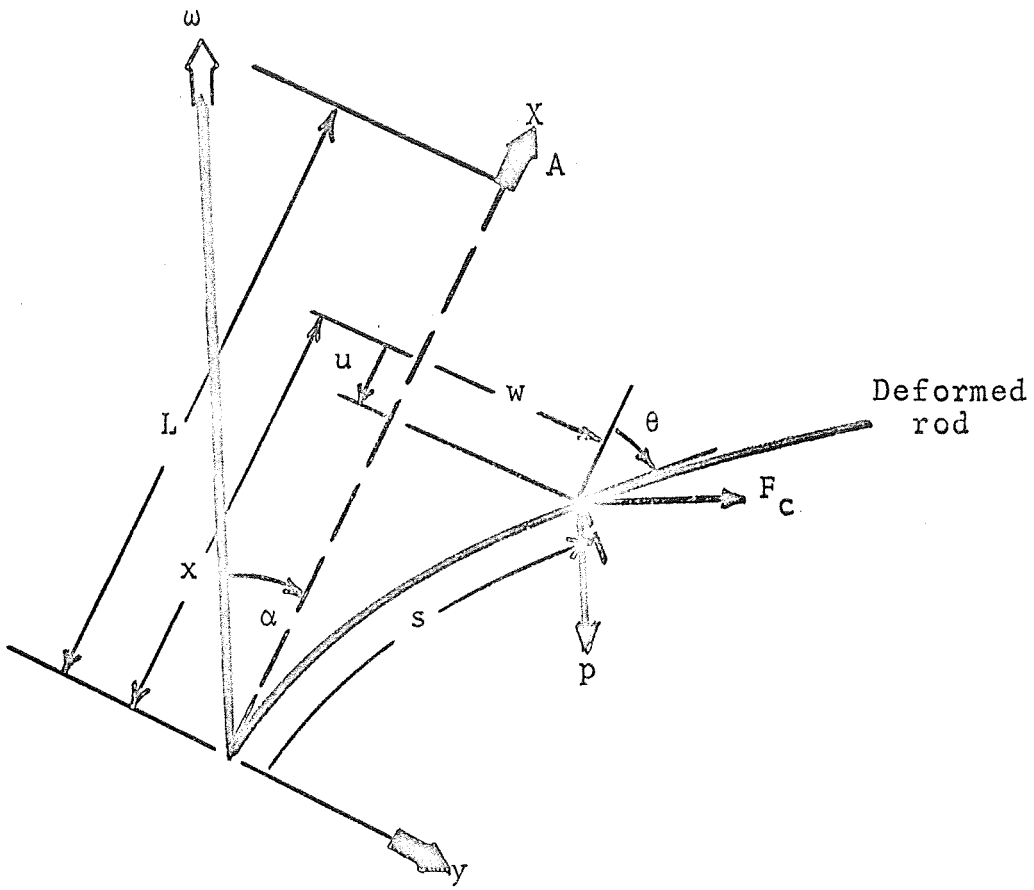

Figure III-1a

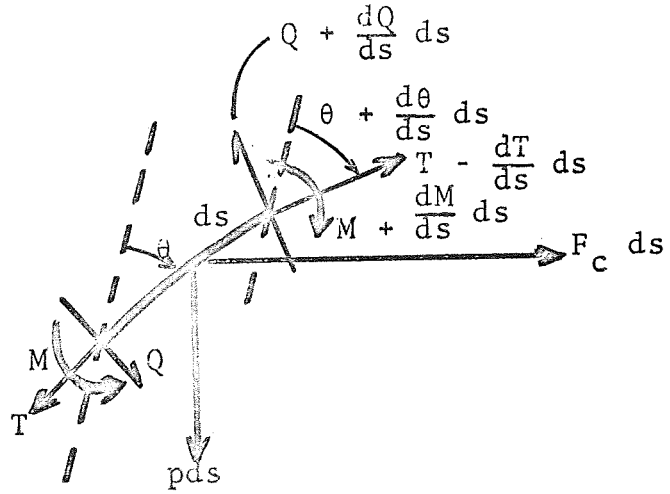

Figure III-1b

Figure III-1. Geometry of Deformation of Slender Rod

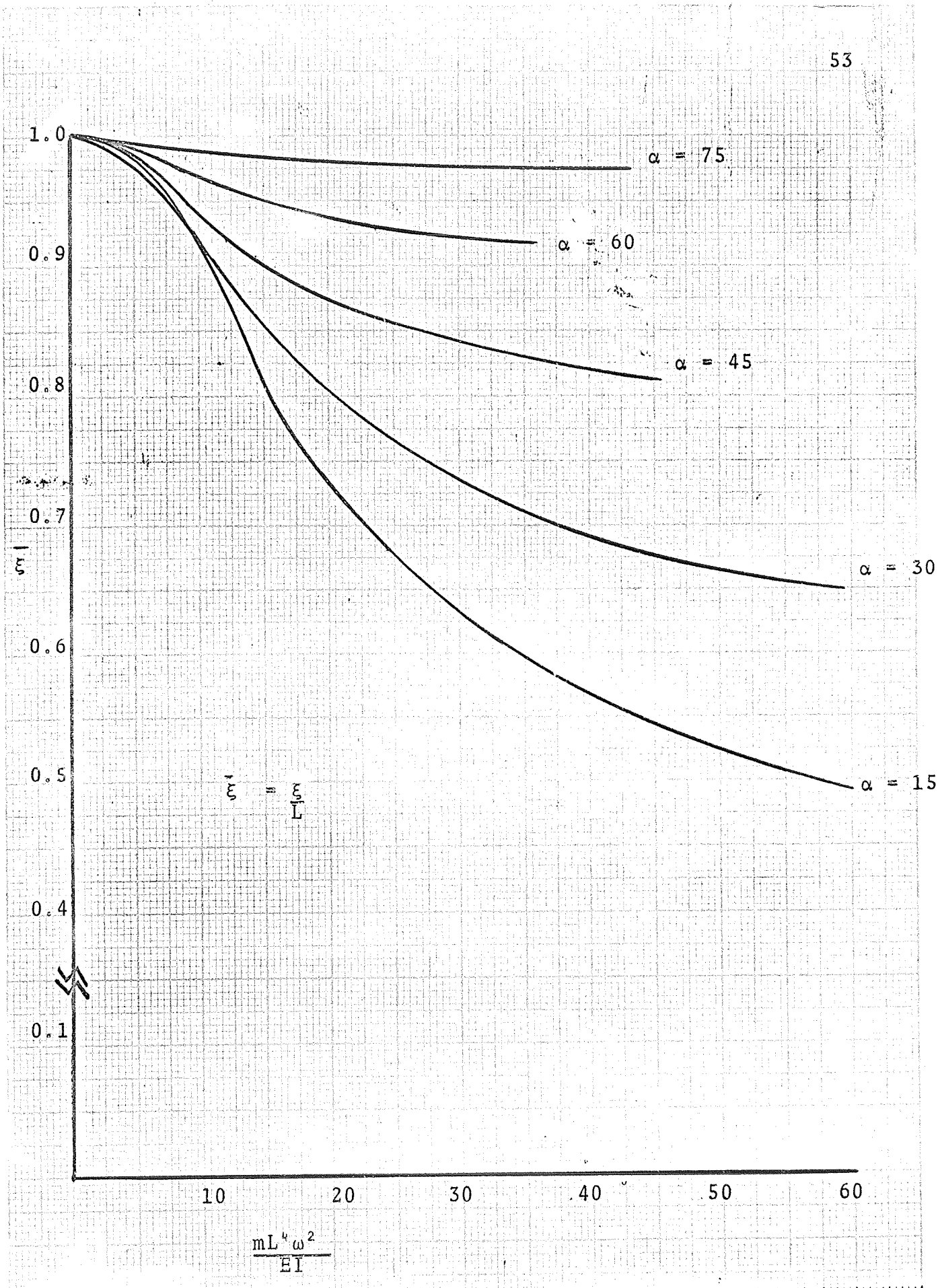

Figure III-2a. Variation in end shortening with angular velocity

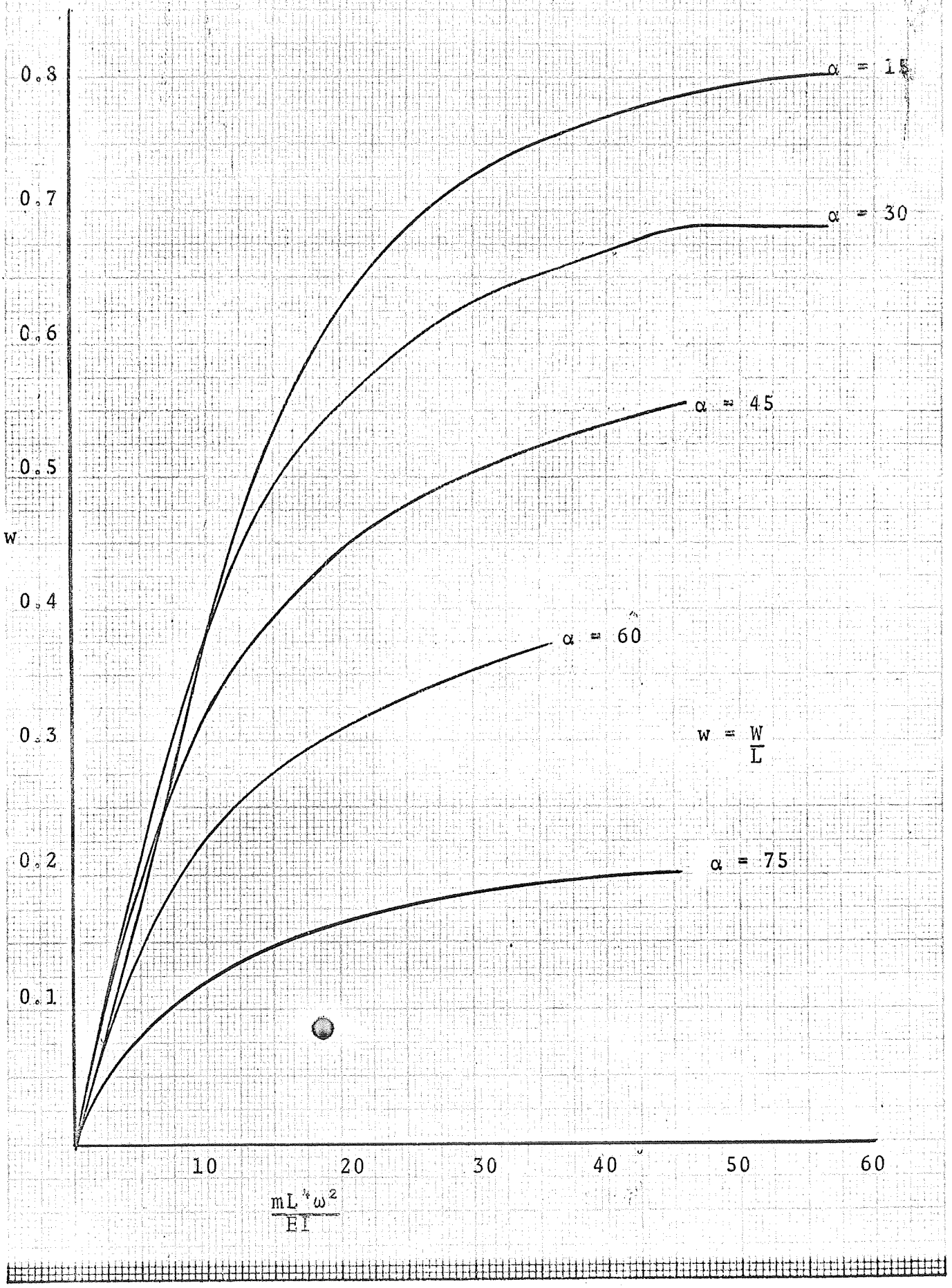

Figure III-2b. Variation in tip deflection with angular velocity

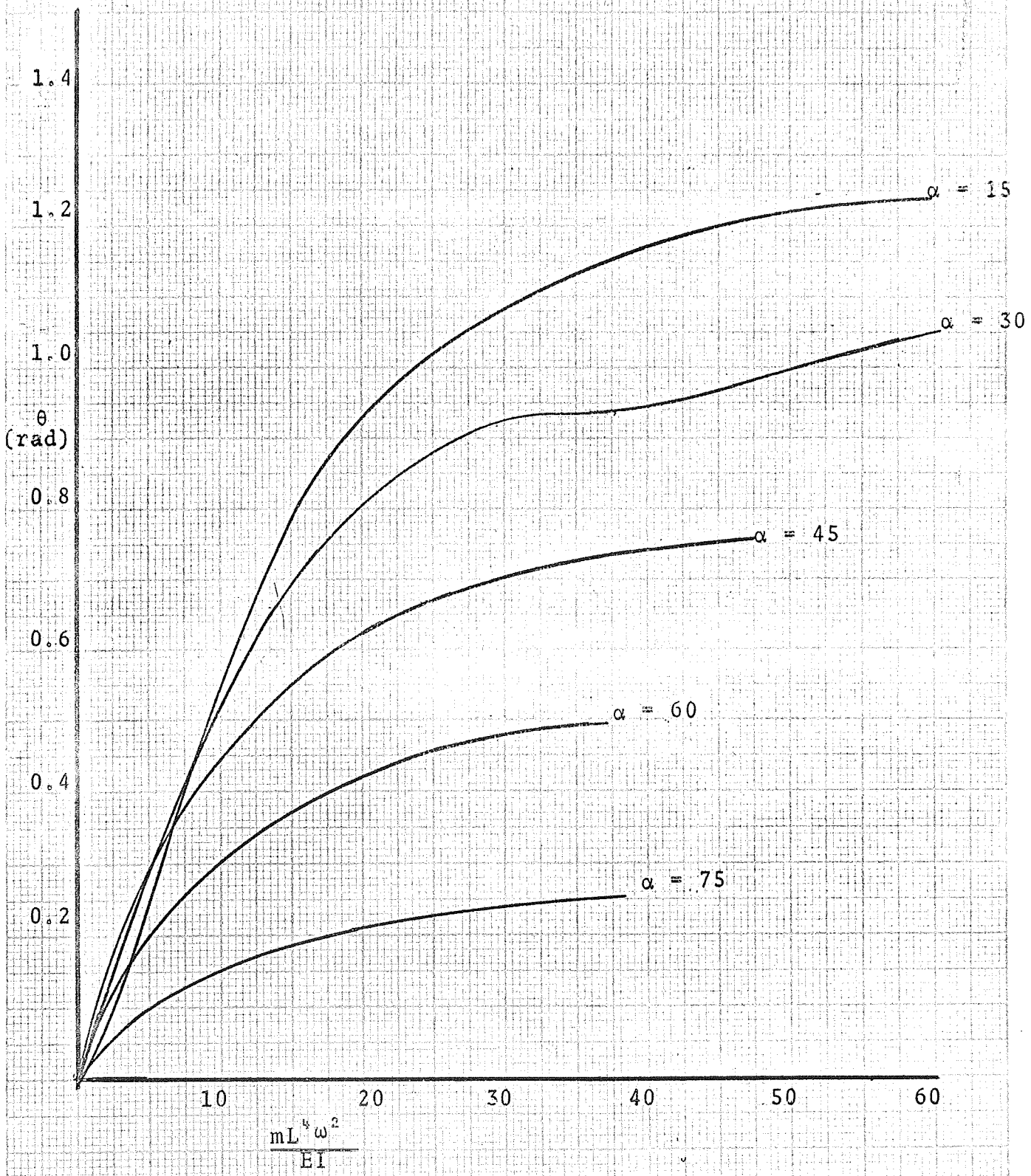

Figure III-2c. Variation in slope at free end with angular velocity

TENSION (TL^2/EI)

$mL^4\omega^2/EI$	$\alpha = 15^0$	$\alpha = 30^0$	$\alpha = 45^0$	$\alpha = 60^0$	$\alpha = 75^0$
0.557	0.0458	0.0717	0.1419	0.2107	0.2603
2.23		0.3132	0.5926	0.8627	1.0473
5.01	0.2037	0.7999	1.4319	1.9910	2.3707
8.91	0.5854	1.6045	2.6839	3.6121	4.2344
13.92	1.1366	2.7270	4.3499	5.7236	6.6376
20.04	1.8484	4.1398	6.4153	8.3193	9.5791
27.27	2.6984	5.8281	8.8738	11.3967	13.0579
35.62	3.6838	7.7954	11.7200		17.0737
45.08	4.8074	10.0228	14.9532	14.9534	21.6266
55.66	6.0760	12.5177			
67.85	7.4721				

Table III-1a. Variation of Fixed End Tension with Angular Velocity

Moment (ML/EI)

$mL^4\omega^2/EI$	$\alpha = 15^0$	$\alpha = 30^0$	$\alpha = 45^0$	$\alpha = 60^0$	$\alpha = 75^0$
0.557	0.1139	0.0821	0.0926	0.0786	0.0477
2.23	0.4984	0.3465	0.3655	0.2933	0.1614
5.01		0.8188	0.7788	0.5892	0.3142
8.91	1.3106	1.4408	1.2546	0.9097	0.4756
13.92	2.1907	2.0908	1.7307	1.2259	0.6340
20.04	3.018	2.7106	2.1891	1.5309	0.7857
27.27	3.7230	3.2981	2.6276	1.8251	0.9341
35.62	4.4821	3.8585	3.056	2.1134	1.0798
45.08	5.1644	4.4136	3.4783		1.2224
55.66	5.8301	4.9623			
67.85	6.4907				

Table III-1b. Variation of Fixed End Bending Moment With Angular Velocity

Appendix

The complete expansions of equations (11) as used in this analysis are

$$\theta(\xi) = \theta(0) + \xi\theta'(0) + \frac{\xi^2}{2!}\theta''(0) + \frac{\xi^3}{3!}\theta'''(0) + \frac{\xi^4}{4!}\theta^{IV}(0) + \frac{\xi^5}{5!}\theta^5(0) + \frac{\xi^6}{6!}\theta^6(0) + \frac{\xi^7}{7!}\theta^7(0) + \frac{\xi^8}{8!}\theta^8(0) + \frac{\xi^9}{9!}\theta^9(0) + \frac{\xi^{10}}{10!}\theta^{10}(0) \tag{A1}$$

$$F_c(\xi) = F_c(0) + \xi F_c'(0) + \frac{\xi^2}{2}F_c''(0) + \frac{\xi^3}{3!}F_c'''(0) + \frac{\xi^4}{4!}F_c^{IV}(0) + \frac{\xi^5}{5!}F_c^5(0) + \frac{\xi^6}{6!}F_c^6(0) + \frac{\xi^7}{7!}F_c^7(0) + \frac{\xi^8}{8!}F_c^8(0) + \frac{\xi^9}{9!}F_c^9(0) + \frac{\xi^{10}}{10!}F_c^{10}(0) + \frac{\xi^{11}}{11!}F_c^{11}(0)$$

where ξ = L-s and Arabic numericals are used to indicate derivatives of $\theta(0)$ and $F_c(0)$ higher than the fourth.

By successive differentiation of the equations

$$\frac{d\theta}{d\xi} = -M/B \tag{A2}$$

$$\frac{d^2\theta}{d\xi^2} = -\frac{1}{B}\frac{dM}{d\xi} = \frac{Q}{B}$$

it is seen that the tenth derivative of $\theta(0)$ with respect to s can be written as

$$\frac{d^{10}\theta(0)}{d\xi^{10}} = \frac{1}{B}\frac{d^{8}Q}{d\xi^{8}} \qquad \text{(A3)}$$

so that terms up to the eighth derivative of Q are needed.

The corresponding nonzero derivatives of $\theta(0)$ and $F_c(0)$ are these listed as follows. Note that it is necessary that the sequence of differentiation be carried out as shown in order that the succeeding terms in the sequence are defined as functions of the previous terms.

$$Q'(0) = -p\sin\beta - F_c(0)\cos\beta$$
$$F_c'(0) = -m_\omega^2 \sin\beta$$
$$T'(0) = -p\cos\beta + F_c(0)\sin\beta$$
$$Q''(0) = -F_c'(0)\cos\beta$$
$$T''(0) = F_c'(0)\sin\beta$$
$$Q^{IV}(0) = Q'(0)\,(3T'(0) - p\cos\beta + F_c(0)\sin\beta)/B$$
$$T^{IV}(0) = (-3Q'(0) + p\sin\beta + F_c(0)\cos\beta)\,Q'(0)/B$$
$$F^{IV}(0) = -m_\omega^2 Q'(0)\cos\beta/B \qquad \text{(A4)}$$
$$T^{5}(0) = (-10Q'(0)\,Q''(0) + pQ''(0)\sin\beta + 3F_c'(0)\,Q'(0)\cos\beta + F_c(0)\,Q''(0)\cos\beta)/B + F_c^{IV}\sin\beta$$
$$Q^{5}(0) = (4T'(0)\,Q''(0) + 6T''(0)\,Q'(0) + Q''(0)\,(-p\cos\beta + F_c(0)\sin\beta) + 4F_c'(0)\,Q'(0)\sin\beta)/B - F_c^{IV}(0)\cos\beta$$
$$F_c^{5}(0) = -m_\omega^2 Q''(0)\cos\beta/B$$
$$Q^{6}(0) = Q''(0)\,(10T''(0) + 5F_c'(0)\sin\beta)/B - F_c^{5}(0)\cos\beta$$
$$Q^{7}(0) = (6T'(0)\,Q^{IV}(0) + 15T^{IV}(0)\,Q'(0) - pQ^{IV}(0)\cos\beta + 10Q'(0)^2\,(p\sin\beta + F_c(0)\cos\beta)/B + F_c(0)\,Q^{IV}(0)\sin\beta)/B$$
$$F^{7}(0) = -m_\omega^2\,(Q^{IV}(0)\cos\beta - 10Q'(0)^2\sin\beta/B)/B$$
$$Q^{8}(0) = (7T'(0)\,Q^{5}(0) + 21T''(0)\,Q^{IV}(0) + 35T^{IV}(0)\,Q''(0))/B - pQ^{5}(0)\cos\beta/B + 35\,(pQ'(0)\,Q''(0)\sin\beta$$

$$+ 2F_c'(0)\, Q''^2(0) \cos\beta + F_c(0)\, Q'(0)\, Q''(0) \cos\beta)/B^2$$

$$+ 35F_c^{IV}(0)\, Q'(0) \sin\beta/B + 7\, F_c'(0)\, Q^{IV}(0) \sin\beta/B$$

$$+ F_c(0)\, Q^5(0) \sin\beta/B - F_c^7(0) \cos\beta + 9T^5(0)\, Q'(0)/B$$

$$F_c^8(0) = -m\omega^2\, (Q^5(0) \cos\beta - 35\, Q'(0)\, Q''(0) \sin\beta/B)B$$

$$F_c^9(0) = -\, m\omega^2\, (Q^6(0) \cos\beta - 35Q''(0)^2 \sin\beta/B)/B$$

$$F^{10}{}_c(0) = m\omega^2\, (-Q^7(0) \cos\beta + 84\, Q'(0)\, Q^{IV}(0) \sin\beta/B$$

$$+ 280\, Q'(0)^3 \cos\beta/B^2)/B$$

$$F_c^{11} = m\omega^2/B\, (-\, Q^8(0) \cos\beta + 36Q^5(0)\, Q'(0) \sin\beta/B$$

$$+ 84Q^5(0)\, Q'(0) \sin\beta/B + 210\, Q^{IV}(0)\, Q''(0) \sin\beta/B$$

$$+ 2100\, Q'(0)^2\, Q''(0) \cos\beta/B^2$$

Therefore, with the weight per unit length (p), mass per unit length m, angle of inclination (α), and bending stiffness (B) defined all terms in equation (A4), and hence in equations (A1) can be calculated

CHAPTER IV

VIBRATIONS OF RODS SUBJECTED TO GYROSCOPIC MOTION

Summary

A set of differential equations and boundary conditions are derived governing the small amplitude vibration behavior of long slender rods and pressurized tubes about a large deflection equilibrium state.* Particular results are obtained numerically for natural frequencies and mode shapes of a cantilever rod inclined to, and rotated about the vertical at a constant angular velocity.

IV-A Introduction

The small amplitude vibration analysis of slender rods and pressurized tubes about large deflection (nonlinear) equilibrium states have received little attention in the literature. This is due mainly to the fact that an accurate description of a nonlinear equilibrium state is difficult to obtain, and even if known, introduces complicated variable coefficients in the linear differential (vibration) equations which makes solution by numerical methods mandatory.

The previous chapter was concerned with the development of an efficient numerical solution for the nonlinear equilibrium state of a slender cantilevered rod, inclined to and rotated about the vertical at a constant angular velocity. The purpose of this chapter is to develop and solve the equations governing the small amplitude vibration behavior about this nonlinear equilibrium state.

---

*here an equilibrium state means a steady state motion or a steady dynamic equilibrium state.

The small deflection, linear vibration equations are derived by a perturbation analysis of the general nonlinear equations presented in (IV-1). The resulting equations are solved by the method of finite differences similar to that presented in (IV-2) and used extensively by the author in (IV-3) with excellent results. For this analysis, because of time considerations, "out of plane", perturbed motion is neglected so that the resulting set of inplane equations becomes a sixth order set of simultaneous differential equations with variable coefficients that are functions of the nonlinear equilibrium state.

The numerical results obtained in this analysis are verified by comparing with the experimental results, obtained from the experimental program carried out in this study and discussed in detail in Chapter V.

IV-B Analysis

In this section, the differential equations are derived which govern the small amplitude vibrational behavior about the equilibrium position of a slender cantilever rod (or pressurized tube) inclined to and rotating about the vertical at a constant angular velocity. In order that this be accomplished, the generalized deflections and internal forces in the vibrating rod are assumed to be made up of (a) those terms associated with an equilibrium state (or steady state motion) and (b) those terms associated with infinitesimal time dependent perturbations about this equilibrium state.

The general nonlinear equations of motion for a slender rod are taken directly from (IV-1) and in that notation are

$$\begin{aligned}
&\frac{dN}{ds} - N'\tau + T\kappa' + X = 0 \\
&\frac{dN'}{ds} - T\kappa + N\tau + Y = 0 \\
&\frac{dT}{ds} - N\kappa' + N'\kappa + Z = 0 \\
&\frac{dG}{ds} - G'\tau + H\kappa' - N' + K = 0 \\
&\frac{dG'}{ds} - H\kappa + G\tau + N + K' = 0 \\
&\frac{dH}{ds} - G\kappa' + G'\kappa + \theta = 0
\end{aligned} \tag{1}$$

where G and G' are the bending moments, H is the twisting moment, and N and N' and the transverse shears. These quantities are shown in the freebody in Figure IV-2. In comparison with the notation of the previous chapter G and N' are respectively M and Q i.e., the "inplane" bending moment and transverse shear force. If shear deformation is neglected, the moments are related to the curvatures by the relations

$$G = B\kappa \qquad G' = B\kappa' \qquad H = C\tau \tag{2}$$

where B is the bending stiffness and C is the twisting stiffness.

The equilibrium state, denoted by a subscript zero, for the inclined cantilevered rod rotating at a constant angular velocity about the vertical is now obtained as a special case of equations (1). In particular, for this steady state case, the "out of plane" bending, transverse shear, and curvature, G', N, κ' are zero as well as the torsion H and twist τ. Then equations (1) reduce to

$$\begin{aligned} \frac{dN_0'}{ds} - \kappa_0 T_0 + Y_0 &= 0 \\ \frac{dT_0}{ds} + \kappa_0 N_0' + Z_0 &= 0 \\ \frac{dG_0}{ds} - N_0' &= 0 \end{aligned} \tag{3}$$

where the curvature $\kappa_0 = \frac{d\theta_0}{ds}$. Equations (3) are identical to equations (8) derived in the Chapter III.

Now to derive the linear vibration equations about the equilibrium state defined by equations (3), the terms appearing in equations (1) are written as

$$\begin{aligned} T &= T_0 + \Delta T \\ H &= H_0 + \Delta H \\ X &= X_0 + \Delta X \\ &\vdots \\ &\text{etc.} \end{aligned} \tag{4}$$

where subscript zero terms refer to the equilibrium state and the incremental values denote infinitesmal time dependent perturbations about the equilibrium state. Substituting equations (4) into equations (1), subtracting out the equilibrium state given by equations (3), and neglecting products of the perturbation terms, the linearized set of vibration equations become

$$\frac{d}{ds}(\Delta N) - N_0'\Delta\tau + T_0\Delta\kappa' + \Delta X = 0$$

$$\frac{d}{ds}(\Delta N') - \kappa_0\Delta T - T_0\Delta\kappa + \Delta Y = 0$$

$$\frac{d}{ds}(\Delta T) + \kappa_0 \Delta N' + N_0' \Delta\kappa + \Delta Z = 0$$

$$\frac{d}{ds}(\Delta G) - \Delta N' + \Delta K = 0$$

$$\frac{d}{ds}(\Delta G') - \kappa_0 \Delta H + G_0 \Delta\tau + \Delta N + \Delta K' = 0 \qquad (5)$$

$$\frac{d}{ds}(\Delta H) - G_0 \Delta\kappa' + \kappa_0 \Delta G' + \Delta\theta = 0$$

where

$$\Delta\kappa = \frac{-d^2 v}{ds^2} + \frac{d}{ds}(w\kappa_0)$$

$$\Delta\kappa' = -\beta\kappa_0 + \frac{d^2 u}{ds^2} \qquad (6)$$

$$\Delta\tau = \frac{d\beta}{ds} + \kappa_0 \frac{du}{ds}$$

and

$$\Delta G = B\Delta\kappa$$

$$\Delta G' = B\Delta\kappa' \qquad (7)$$

$$\Delta H = C\Delta\tau$$

$$\Delta T = EA\left(\frac{dw}{ds} + \frac{G_0}{B} v\right)$$

The last terms in each of equations (5) are due to the change in the applied external loads during the deformation of the rod away from its equilibrium state. For this case of the rod rotating about the vertical, the applied external loads considered here are due to (a) the uniformly distributed weight of the rod itself and (b) the "reverse effective forces" due to the acceleration of the rod.

If rotary inertia is neglected and there are no uniformly distributed couples along the length of the rod, then

$$\Delta K = \Delta K' = \Delta\theta = 0 \tag{8}$$

The contribution of the remaining accelerational forces to ΔX, ΔY, ΔZ are now obtained. Consider the inertial XYZ coodinate system shown in Figure IV-1. In addition, a body fixed set of axis x, y, z are oriented as shown in the tangential, normal, and binormal direction with respect to the deformed equilibrium state. For steady state motion due to a constant angular velocity it is obvious that the "accelerational force" is just

$$\vec{F}_{accel} = -m\,\vec{\omega} \times \vec{\omega} \times \vec{R} \tag{9}$$

where

$$\vec{\omega} = -\vec{j}\omega \sin(\alpha + \theta_0) + \vec{k}\omega \cos(\alpha + \theta_0) \tag{10}$$

and $\vec{R}$ is the radius vector to the origin of the body fixed coordinate system in the equilibrium state. If equation (9) is expanded the resulting force due to this centrifugal acceleration is the same as that obtained in the previous chapter, i.e.,

$$Z_{0_{accel}} = F_c \sin(\alpha + \theta_0)$$

$$Y_{0_{accel}} = F_c \cos(\alpha + \theta_0)$$

where F_c is the centrifugal force vector perpendicular to the axis of rotation and is defined by equation (9).

The acceleration of point 0 away from the equilibrium state can be written as

$$\vec{a}_0 = \vec{a} + 2\vec{\omega} \times \vec{V} + \vec{\omega} \times \vec{\omega} \times \vec{r} \qquad (11)$$

where

$$\vec{a} = \vec{i}\,\ddot{u} + \vec{j}\,\ddot{v} + \vec{k}\,\ddot{w}$$

$$\vec{V} = \vec{i}\,\dot{u} + \vec{j}\,\dot{v} + \vec{k}\,\dot{w} \qquad (12)$$

$$\vec{r} = \vec{i}\,u + \vec{j}\,v + \vec{k}\,w$$

$$\vec{\omega} = 0 - \vec{j}\omega \sin(\alpha + \theta_0) + \vec{k}\omega \cos(\alpha + \theta_0)$$

and dots over the symbols indicate differentiation with respect to time. Note that the perturbation displacements u, v, w are in the binormal, normal, and tangential directions respectively with respect to the deformed state. Thus, the change in forces in the x, y, z, directions due to the acceleration are obtained by substituting equations (12) into (11), expanding and multiplying the result by the mass m. Then

$$\Delta X_{accel} = -m\left[\ddot{u} - u\omega^2 - \omega(\dot{w}\sin(\alpha + \theta_0) + \dot{v}\cos(\alpha + \theta_0))\right]$$

$$\Delta Y_{accel} = -m\left[\ddot{v} - \omega^2\cos(\alpha + \theta_0)(w\sin(\alpha + \theta_0) + v\cos(\alpha + \theta_0)) + \omega\dot{u}\cos(\alpha + \theta_0)\right]$$

$$\Delta Z_{accel} = -m\left[\ddot{w} - \omega^2\sin(\alpha + \theta_0)(w\sin(\alpha + \theta_0) + v\cos(\alpha + \theta_0)) + \omega\dot{u}\sin(\alpha + \theta_0)\right] \qquad (13)$$

In addition to the accelerational forces, the applied external loads may also change during the deformation of the rod away from its equilibrium state. For this analysis consider the rod to be loaded uniformly by its own weight. In the equilibrium state, the components of force due to the weight pds of a differential element ds at point 0 are, in the positive z direction:

$$Z_{0_{weight}} = -p\cos(\alpha + \theta_0) \qquad (14)$$

in the positive y direction

$$Y_{0_{weight}} = p \sin (\alpha + \theta_0) \tag{14}$$

However, as point 0 moves to point $0'$ the components of force change to:

in the positive z' direction

$$Z_{0_{weight}} + \Delta Z_{weight} = p \cos (\alpha + \theta_0 + \Delta\theta)$$

in the positive y' direction (15)

$$Y_{0_{weight}} + \Delta Y_{weight} = p \sin (\alpha + \theta_0 + \Delta\theta)$$

where $\Delta\theta$ is the inplane rotation of the axis system xyz with respect to $x'y'z'$, the later being tangent and normal to the perturbed configuration at $0'$. Expanding equation (15), assuming $\Delta\theta$ small compared to unity, and subtracting out the identities (14), the net change in the external loads due to the deformation of the rod away from equilibrium becomes

$$\begin{aligned} \Delta X_{weight} &= 0 \\ \Delta Z_{weight} &= p\Delta\theta \sin(\alpha + \theta_0) \\ \Delta Y_{weight} &= p\Delta\theta \cos(\alpha + \theta_0) \end{aligned} \tag{16}$$

where

$$\Delta\theta = -\left(-\frac{dv}{ds} + \frac{G_0}{B} w\right) \tag{17}$$

Now substituting equations (8), (13), and (16) into equations (5), we obtain the linearized vibration equations for the rod.

$$\frac{d}{ds}(\Delta N) - N_0'\Delta\tau + T_0\Delta\kappa' - m\left[\ddot{u} - u\omega^2 - \omega(\dot{w}\sin(\alpha + \theta_0) + \dot{v}\cos(\alpha + \theta_0))\right] = 0$$

$$\frac{d}{ds}(\Delta N') - \kappa_0\Delta T - T_0\Delta\kappa + p\Delta\theta\cos(\alpha + \theta_0) - m\left[\ddot{v} - \omega^2\cos(\alpha + \theta_0)(w\sin(\alpha + \theta_0) + v\cos(\alpha + \theta_0)) + \omega\dot{u}\cos(\alpha + \theta_0)\right] = 0$$

$$\frac{d}{ds}(\Delta T) + \kappa_0\Delta N' + N_0'\Delta\kappa + p\Delta\theta\sin(\alpha + \theta_0) - m\left[\ddot{w} - \omega^2\sin(\alpha + \theta_0)(w\sin(\alpha + \theta_0) + v\cos(\alpha + \theta_0)) + \omega\dot{u}\sin(\alpha + \theta_0)\right] = 0$$

$$\frac{d}{ds}(\Delta G) - \Delta N' = 0 \tag{18}$$

$$\frac{d}{ds}(\Delta G') - \kappa_0\Delta H + G_0\Delta\tau + \Delta N = 0$$

$$\frac{d}{ds}(\Delta H) - G_0\Delta\kappa' + \kappa_0\Delta G' = 0$$

Making use of equations (2) and (7) in equations (18) there results, for a rod of constant cross section,

$$C\frac{d}{ds}(\Delta\tau) - G_0\Delta\kappa' + \frac{G_0'}{B}B\Delta\kappa' = 0 \qquad (19)$$

or since the twisting stiffness C is not zero

$$\frac{d}{ds}(\Delta\tau) = 0 \quad \Rightarrow \quad \Delta\tau = \text{constant} \qquad (20)$$

However, for the case being investigated, it is obvious that the change in twist at the free end is zero and thus by equation (20), the change in twist is identically zero throughout the length of the rod.

In a similar manner substituting equations (2) and (7) into the fifth equation of equations (18) yields the following relation between the "out of plane" shear and bending moment

$$\frac{d}{ds}(\Delta G') + \Delta N = 0 \qquad (21)$$

It should be noticed that this same result is obtained if equation (20) is substituted into the fifth equation of equations (18).

Now using equations (20), (21) and the fourth equation of equations (18) in the first three equations of equations (18), we obtain

$$- \frac{d^2}{ds^2}(\Delta G') + \frac{T_0}{B}\Delta G' - m\left[\ddot{u} - \omega^2 u - \omega(\dot{w}\sin(\alpha + \theta_0) + \dot{v}\cos(\alpha + \theta_0))\right] = 0$$

$$\frac{d^2}{ds^2}(\Delta G) - \frac{G_0}{B}\Delta T - \frac{T_0}{B}\Delta G - p(-\frac{dv}{ds} + \frac{G_0}{B}w)\cos(\alpha + \theta_0) -$$

$$m\left[\ddot{v} - \omega^2\cos(\alpha + \theta_0)(w\sin(\alpha + \theta_0) + v\cos(\alpha + \theta_0)) + \omega\dot{u}\cos(\alpha + \theta_0)\right] = 0$$

$$\frac{d}{ds}(\Delta T) + \frac{G_0}{B}\frac{d}{ds}(\Delta G) + \frac{N_0'}{B}\Delta G - p(-\frac{dv}{ds} + \frac{G_0}{B}w)\sin(\alpha + \theta_0)$$

$$-m\left[\ddot{w} - \omega^2\sin(\alpha + \theta_0)(w\sin(\alpha + \theta_0) + v\cos(\alpha + \theta_0)) + \omega\dot{u}\sin(\alpha + \theta_0)\right] = 0 \qquad (22)$$

Equations (6), (7), (22), and the boundary conditions

at $s = 0$ $\qquad u = v = w = \Delta\theta = \frac{dw}{ds} = 0$

and at $s = L$ $\qquad \Delta G = \Delta G' = \Delta N = \Delta N' = \Delta T = 0$

constitute a well defined eigenvalue problem for the infinitesmal vibrations of a thin cantilever rod inclined to and rotated about the vertical at a constant angular velocity.

Eigenvalue Problem

Because of time limitations, it was necessary to restrict attention only to the "inplane" vibration equations. These are obtained directly from equations (22) by neglecting the out of plane perturbation displacement u. The resulting set of equations to be solved are

$$\frac{d^2}{ds^2}(\Delta G) - \frac{G_0}{B}\Delta T - \frac{T_0}{B}\Delta G - p\cos(\alpha + \theta_0)\left(-\frac{dv}{ds} + \frac{G_0}{B}w\right)$$
$$- m\left[\ddot{v} - \omega^2\cos(\alpha + \theta_0)\left(w\sin(\alpha + \theta_0) + v\cos(\alpha + \theta_0)\right)\right] = 0$$

$$\frac{d}{ds}(\Delta T) + \frac{G_0}{B}\frac{d}{ds}(\Delta G) + \frac{N_0'}{B}\Delta G - p\sin(\alpha + \theta_0)\left(-\frac{dv}{ds} + \frac{G_0}{B}w\right)$$
$$- m\left[\ddot{w} - \omega^2\sin(\alpha + \theta_0)\left(w\sin(\alpha + \theta_0) + v\cos(\alpha + \theta_0)\right)\right] = 0$$

$$\Delta T - EA\left(\frac{dw}{ds} + \frac{G_0}{B}v\right) = 0 \qquad (23)$$

$$-\Delta G/B - \frac{d^2v}{ds^2} + \frac{d}{ds}\left(\frac{G_0}{B}w\right) = 0$$

subject to the boundary conditions

$$\text{at } s = 0 \qquad v = w = \Delta\theta = 0$$
$$(24)$$
$$\text{at } s = L \qquad \Delta T = \Delta G = \Delta N' = 0$$

Reduction to ordinary differential equations. Since equations (23) are partial differential equations and the solution, in general, can only be achieved by numerical techniques, the procedure of (IV-2) is adopted where the dependence on time is eliminated by assuming simple harmonic motion and introducing G as an additional unknown. This procedure yields a set of three coupled second-order differential equations with variable coefficients that are functions of the equilibrium state. Thus, substituting the third equation of equations (23) into the first and second equations of equations (23) and assuming the simple harmonic motion defined by

$$v = v(s)\, e^{i\Omega t}$$

$$w = w(s)\, e^{i\Omega t} \qquad (25)$$

$$\Delta G = \Delta G(s)\, e^{i\Omega t}$$

the governing equations of motion became

$$F_{13} \frac{d^2}{ds^2}(\Delta G) + G_{11}\frac{dv}{ds} + G_{12}\frac{dw}{ds} + H_{11}v + H_{12}v + H_{13}\Delta G = 0$$

$$F_{22}\frac{d^2w}{ds} + G_{21}\frac{dv}{ds} + G_{23}\frac{d(\Delta G)}{ds} + H_{21}v + H_{22}w + H_{23}\Delta G = 0$$

$$F_{31}\frac{d^2}{ds^2}(\Delta G) + G_{31}\frac{dv}{ds} + G_{23}\frac{d}{ds}(\Delta G) + H_{32}w + H_{33}\Delta G = 0 \qquad (26)$$

The last equation of equations (26) is the equation for the moment ΔG in terms of the displacements. The subscripted coefficients in equations (26) are defined as

$$F_{11} = 0 \qquad G_{11} = A_1 \qquad H_{11} = -\left(\frac{G_0}{B}\right)^2 EA + m\omega^2\cos^2(\alpha + \theta_0) + m\Omega^2$$

$$F_{12} = 0 \qquad G_{12} = -\frac{G_0}{B} EA \qquad H_{12} = m\omega^2\sin(\alpha + \theta_0)\cos(\alpha + \theta_0) - \frac{G_0}{B}A_1$$

$$F_{13} = 1 \qquad G_{13} = 0 \qquad H_{13} = -T_{0/B}$$

$$F_{21} = 0 \qquad G_{21} = EA\,\frac{G_0}{B} + A_2 \qquad H_{21} = \frac{EA}{B} N_0' + m\omega^2 \sin(\alpha + \theta_0)\cos(\alpha + \theta_0)$$

$$F_{22} = EA \qquad G_{22} = 0 \qquad H_{22} = m\Omega^2 + m\omega^2 \sin(\alpha + \theta_0) - A_2\,\frac{G_0}{B}$$

$$F_{23} = 0 \qquad G_{23} = \frac{G_0}{B} \qquad H_{23} = \frac{N_0'}{G}$$

$$F_{31} = 1 \qquad G_{31} = 0 \qquad H_{31} = 0$$

$$F_{32} = 0 \qquad G_{32} = \frac{G_0}{B} \qquad H_{32} = \frac{N_0'}{B}$$

$$F_{33} = 0 \qquad G_{33} = 0 \qquad H_{33} = -1/B \qquad (27)$$

$$A_1 = p\cos(\alpha + \theta_0) \qquad A_2 = p\sin(\alpha + \theta_0)$$

In a similar manner, the boundary conditions (eqns. 24) can be written as

$$e_{13}\frac{d(\Delta G)}{ds} = 0 \qquad \text{or} \quad v = 0$$

$$e_{22}\frac{dw}{ds} + f_{21} = 0 \qquad \text{or} \quad w = 0 \qquad (28)$$

$$e_{31}\frac{dv}{ds} + f_{32} = 0 \qquad \text{or} \quad \Delta G = 0$$

where the nonzero coefficients are

$$e_{13} = 1 \qquad f_{21} = \frac{EA}{B} G_0 \qquad e_{31} = -1$$
$$e_{22} = EA \qquad f_{32} = G_0/B \tag{29}$$

Numerical procedure. The numerical procedure for the solution of equations (26) is as follows. The length of the rod is divided into equal increments and a three point central difference formula is used to reduce the differential equations to algebraic form. The three point difference formulas at the ith station are

$$Z_i'' = \frac{1}{\Delta^2} (Z_{i-1} - 2Z_i + Z_{i+1})$$
$$Z_i' = \frac{1}{2\Delta} (-Z_{i-1} + Z_{i+1}) \tag{30}$$

where Δ is the length of the interval $s_i - s_{i-1}$ and primes now denote differentiation with respect to s. Now define the vector Z as

$$Z_i = \begin{Bmatrix} v \\ w \\ \Delta G \end{Bmatrix}_i \tag{31}$$

so that equations (26) may be written as

$$F_i Z_i'' + G_i Z_i' + H_i Z_i = 0 \tag{32}$$

where the F_i, G_i, and H_i are each 3 x 3 matrices defined at each station along the rod.

In a similar manner, if the vector N is defined as

$$N_i = \left\{ \begin{matrix} \Delta N' \\ \Delta T \\ \Delta \theta \end{matrix} \right\}_i \tag{33}$$

the general boundary conditions for a rod can be written as

$$\alpha_{ij} N_j + \beta_{ij} Z_j = 0 \tag{34}$$

where the α_{ij} and β_{ij} are each 3 x 3 matrices used to select the prescribed boundary conditions. Using the last two of equations (23) together with equations (17) and the fourth equation of equations (18) in (33) yields the general form of the boundary conditions from (34).

$$\begin{aligned} &\alpha_1 e_1 Z_1' + (\alpha_1 f_1 + \beta_1) Z_1 = 0 \quad \text{at } i = 1 \\ &\alpha_m e_m Z_m' + (\alpha_m f_m + \beta_m) Z_m = 0 \quad \text{at } i = m \end{aligned} \tag{35}$$

For the fixed free boundary conditions given by equations (24) the nonzero coefficients in α and β matrices at i = 1 and m are

$$\begin{aligned} &\text{at } i = 1 && \alpha_{33} = \beta_{11} = \beta_{22} = 1 \\ &\text{at } i = m && \alpha_{11} = \alpha_{22} = \beta_{33} = 1 \end{aligned} \tag{36}$$

Now applying equations (30) to equations (32) and (35), the governing equations become

$$A_i Z_{i-1} + B_i Z_i + C_i Z_{i+1} = 0 \tag{37}$$

where

$$\begin{aligned} A_i &= \frac{F_i}{\Delta^2} - \frac{G_i}{2\Delta} \\ B_i &= H_i - \frac{2F_i}{\Delta^2} \\ C_i &= \frac{F_i}{\Delta^2} + \frac{G_i}{2\Delta} \end{aligned} \tag{38}$$

The corresponding boundary conditions are

$$\begin{aligned} &\frac{\alpha_0 e_0}{2\Delta}(-Z_0 + Z_2) + (\alpha_0 f_0 + \beta_0) Z_1 = 0 \\ &\frac{\alpha_m e_m}{2\Delta}(-Z_{m-1} + Z_{m+1}) + (\alpha_m f_m + \beta_m) Z_m = 0 \end{aligned} \tag{39}$$

The off-boundary points Z_0 and Z_{m+1} are eliminated by substituting equations (37) into (39) so that the boundary conditions are now written in the convenient form

$$D_1 Z_1 + E_1 Z_2 = 0 \qquad \text{at } i = 1$$

$$E_m Z_{m-1} + D_m Z_m = 0 \text{ at } i = m \tag{40}$$

where

$$D_1 = \alpha_0 \left[\frac{e_0}{2\Delta} A_1^{-1} B_1 + f_0 \right] + \beta_0$$

$$E_1 = \frac{\alpha_0 e_0}{2\Delta} \left[A_1^{-1} C_1 + I \right]$$

$$D_m = \alpha_m \left[\frac{-e_m}{2\Delta} C_m^{-1} B_m + f_m \right] + \beta_m$$

$$E_m = -\frac{\alpha_m e_m}{2\Delta} \left[C_m^{-1} A_m + I \right]$$

Equations (37) written at $i = 2, m-1$ together with equations (40) form a complete set of homogeneous field equations governing the natural frequencies of the cantilever rod. A recursion formula for the Z_i may be obtained from the equation

$$Z_i + P_i Z_{i+1} = 0 \tag{42}$$

where P_i is a 3 x 3 matrix. From equation (40)

$$P_1 = D_1^{-1} E_1 \tag{43}$$

and in general, from equation (37)

$$P_i = (B_i - A_i P_{i-1})^{-1} \tag{44}$$

Writing equation (44) at all points along the rod, we have, at i = m

$$| D_m - E_m P_{m-1} | Z_m = 0 \tag{45}$$

Therefore, any value of Ω which satisfies equation (45) is a natural frequency of the system. These frequencies can be found by selecting successive values of Ω until the determinant of the coefficients of Z_m in equation (45) vanish.

Discussion of Results

Natural frequencies and mode shapes have been calculated for several rod configurations using the numerical technique previously discussed. The results are presented in Table IV-1. All calculation are for a circular cross section rod 34 inches long with a Youngs modulus of $30*10^6$ psi and specific weight of 0.282 $lb/in.^3$.

Several important facts are immediately apparent from the data presented in the table. First it is seen that the natural frequencies are functions of the angle of inclination of the rod from the vertical. In particular, the frequencies decrease as the rod is rotated from the horizontal to the vertical, this decrease being more pronounced as the rod diameter becomes smaller, i.e., more flexible.

Second, it is seen that the frequencies are also functions of the angular velocity of the rod about the vertical. For instance, for the relatively stiff (0.096 in diam.) rod, the frequency increases only 1 cps in the second mode when going from 20 to 40 RPM. However for the more flexible (0.064 in. diam.) rod the frequency increases in the second mode from 22 to 35 cps as the RPM is increased from 20 to 40 RPM. In general, the more flexible the rod, the greater the change in frequency with RPM for any given mode. Likewise for rods of the same flexibility, the frequency change with RPM decreases with an increase in the number of modes.

Diameter (in)	RPM	Weight Included	Mode	α (deg)	Frequency (cps)	Classical Frequency (cps)
0.064"	0	yes	2	90^0	26	62
	0	yes	2	30^0	18	62
	20	yes	2	30^0	22	62
	20	no	1	30^0	10	10
	40	yes	2	30^0	35	62
	40	no	1	30^0	18	10
0.096"	0	yes	1	90^0	18	15
	0	yes	1	30^0	15	15
	20	yes	1	30^0	16	15
	20	yes	2	30^0	92	91
	40	yes	1	30^0	19	15
	40	yes	2	30^0	93	91

TABLE IV-1. Natural Frequencies of Cantilever Rods

Finally, it is noticed that the frequency of the rod is a function of its weight, for the same flexibility. This can be seen from the fact that for the 0.064 in. diameter rod at 20 RPM, the natural frequency changes from 10 to 22 cps, depending on whether the weight is or is not considered.

For the three cases mentioned, the frequency changes with inclination, RPM, and weight, can be attributed directly to the change in the geometric shape of the rod caused by these conditions. In the classical linear theory of vibrations, it is assumed that the vibrations of the rod occur away from an undeformed (straight line) state. However, the results of this analysis show that if the deformations of the rod in the equilibrium state become sufficiently large, the frequencies can change markedly from that predicted by classical theory. The dividing line between "small" and "sufficiently large" deformations as regards to the effect on the frequency changes are not well defined at this time. However, indications are that the sensitivity of the frequency to the geometric shape occurs when the deformations of the equilibrium state as given by linear and nonlinear theory begin to diverge. This statement is borne out in part by the results obtained for the 0.064" and 0.096" rod given in Table IV-1. For the 0.096" rod the deformations as predicted by linear and nonlinear theory are practically the same for the given RPM loading and accordingly, the frequency values obtained using the more exact theory of this analysis differs little from the classical small deflection vibration analysis where the change in geometric shape

prior to vibration is neglected. However, for the 0.064" rod, the deformations as predicted by linear and nonlinear theory differ by about 50% and accordingly, the values of Ω as calculated with the more exact theory of this analysis differs significantly in some cases, with that obtained by classical analysis.

Additional calculations were also made to try to determine the natural frequencies of a 0.032" diameter rod in order to further isolate the effect of the equilibrium state configuration on these natural frequencies. However, it was found that for this case, (and even for some of the case presented in Table IV-1) and in general for any case where the frequencies change markedly with geometric shape; that the values of the calculated natural frequencies were extremely sensitive to the description of the equilibrium state. In other words, when the generalized internal forces and deflections are determined numerically for the equilibrium state, the percentage difference in the results obtained by using say 34 or 68 stations along the length was negligible. However, when these results were substituted into the vibration program, the calculated values of the natural frequencies could differ markedly, depending on the flexibility of the rod. In general, as the rods become more and more flexible, the effect of the equilibrium configuration on the frequencies become more important and thus, a very accurate description of this equilibrium configuration is necessary to obtain reliable values of frequency. For the 0.032" diameter rod, such accuracy could not be obtained on the IBM 360-50

with its 32 bit single precision word and double precision calculations were not made. However, a few runs were made on the Univac 1108 and with its 36 bit single precision word, indications are that reliable solutions could be obtained without having to use double precision.

References

IV-1. Love, A. E. H.: A treatise on the Mathematical Theory of Elasticity. Fourth Edition, Dover Publications.

IV-2. Cooper, Paul A.: Vibration and Buckling of Prestressed Shells of Revolution. NASA TN D-3831, March, 1967

IV-3. Weeks, George E.: Generalized Ring Boundary Conditions For Shells of Revolution. Ph.D. Dissertation presented to Dept. of Engineering Mechanics, Virginia Polytechnic Institute, Oct, 1966.

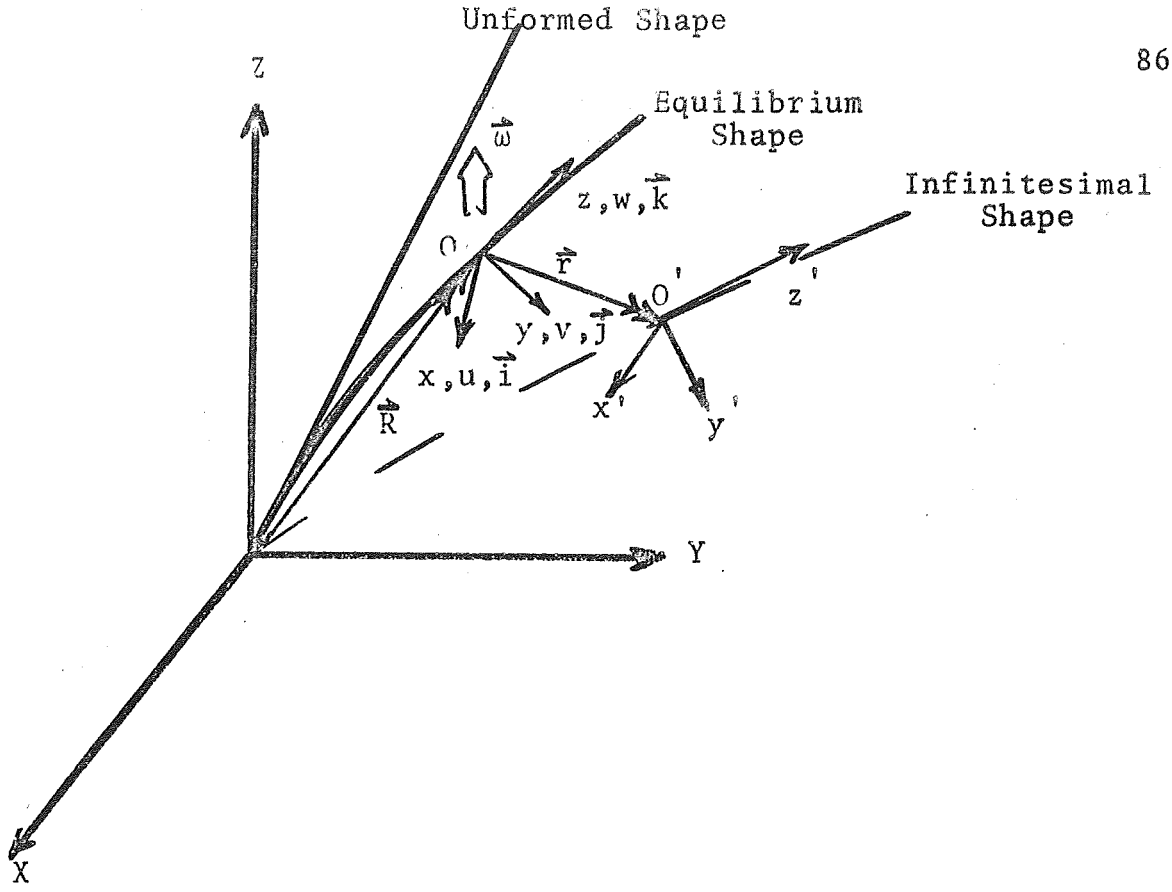

Figure IV-1. Coordinate of Perturbed System

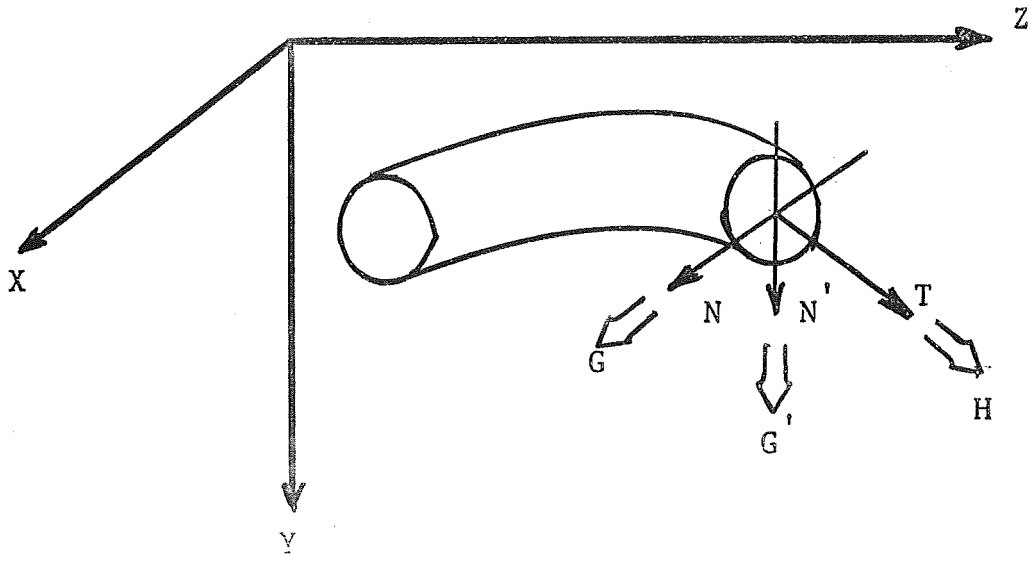

Figure IV-2. Internal Forces and Moments For Three Dimensional Deformation of Rod

CHAPTER V

EXPERIMENTAL RESULTS

Summary

Experimentation was performed on flexible rods subjected to gyroscopic type motion (precession). The experimental set-up is described and results are compared to analytical results discussed in Chapter III. The problems encountered in fabricating and testing of inflated cylinders is discussed.

V-A Flexible Rods

It was desired to experimentally verify the deflections associated with the rotation of the flexible thin rod as predicted by the analytical method developed in Chapter III. To accomplish this, the experimental apparatus shown in Figure V-1 was designed and constructed. Several areas of the design were found to be critical in obtaining acceptable data, principally due to the extreme flexibility of the rods to be tested. The second major source of difficulty in the experimental procedure was the unstabilizing influence of the centrifugal forces generated by rotation of the rod at a deviated angle from the vertical.

Due to the degree of flexibility of the rods, extreme care had to be taken to assure that the angle of incidence was initially accurate, and further, that the angle did not vary during the testing procedure. The first area of concern was in the specimen grip itself. Initially, a bisected rod grip with a milled groove down the center and a tapered thread-locking

device was employed. This proved unsatisfactory, in that the order of locking the sections together tended to shift the actual gripping point on the rod, in effect lengthening the rod and consequently producing erroneous deflection data. Also, this type grip was too heavy, and the centrifugal forces generated in rotating the device were prohibitive with regard to a stable platform. Subsquently, a grip was developed employing chuck collets similar to those used in a jeweler's lathe, with a cap cover providing the force to close the collet. This proved to be an excellent method for gripping the rods, not only from the standpoint of consistent alignment, but also due to the fact that many different size rods could be handled in the same grip merely by changing collets. Some care had to be exercised in installing the rod in the grip to insure a uniformly tight grip (it was found that differences in gripping force produced minute angle changes which became significant as tip deflections) but with a minimum of care, this system proved entirely satisfactory. The matter of constancy of angle during the testing procedure was solved by roughing the surfaces of the joining sections at the angle joint and using a very tight locking screw, double nutted to prevent vibratory loosening. This proved satisfactory, even in rotation ranges where instability of the rods, occurred subjecting the joint to rather severe loadings.

Some problems were encountered due to the centrifugal forces of the rotating rod and grip tending to twist the channel section on which the apparatus was mounted. This was eliminated by additional bracing. These forces also tended to force some wobble

into the system through force on the bearing race for the drive shaft. This was eliminated by installation of a double bearing block and providing the drive force through a gear system rather than directly, forcing the drive shaft into one position.

In taking the deflection data, extreme care was taken to insure accuracy of the angle of incidence. The entire system was leveled within one fiftieth of a degree and the initial angle was adjusted within one tenth of a degree using a precision level instrument before each test. The static deflection data could be taken by direct observation; unfortunately, however, the same cannot be said for the rotational data. Consequently, a photographic method was developed for obtaining the shape and deflection of the rotating rod. A camera was set up in a plane perpendicular to and bisecting the plane in which the deflection was to be measured. The alternative of choosing either exposure or illumination at a prescribed time was resolved by virtue of simplicity. It was found to be much less complicated to illuminate the rod for an extremely short duration at a prescribed instant than to trip the camera shutter under constant illumination at an instant. An electronic system was designed which would trigger an extremely short duration, high intensity flash on any desired revolution of the system, at the exact instant that the rod was in the desired plane. It was then only necessary to darken the laboratory, open the camera shutter, and select the desired revolution of the system to produce a photograph of the deflected rod at any incidence angle and any

angular velocity. A reference length device was also included, in-plane with the rod, in each photograph. From the processed negatives, prints of arbitrary size were made, and, with the use of an opaque projector, actual size reproductions of the deflected rods were drawn. The true size was obtained by comparison with the known reference length as outlined above.

Several critical questions were answered with regard to this system prior to accepting the authenticity of the resultant data from this method. The most serious of these were whether, due to the fact that any lens "sees" spherically, distortions of dimensions would occur with increasing proportion from the center of the rod. These fears were allayed upon measurement of the reproduced arc length of the rod, this length varying less than one half of one per cent from the original. The second question was one of accuracy of the "in-planeness" triggering by the electronic system. This was checked by comparison of several photographs at the same angular velocity. It was reasoned that, if the plane of the rod varied, then the "apparent" deflections in the two dimensional photographs would vary. All of the photographs were, as far as was visually observable, absolutely identical, this serving not only to substantiate the validity of the photographic system, but also to demonstrate the accuracy and stability of the entire experimental apparatus.

Deflection shapes for α= 15 and 30 degrees, ω = 0, 30 and 50 rpm are shown in Figures V-2 and V-3. These are compared with the theoretically predicted shapes developed analytically, all non-dimensionalized using the maximum static deflection as the reference length. It is seen that excellent agreement is obtained,

considerably less than 5% variation at the maximum, a figure considered to be well within the limits of experimental error.

V-B Inflatable Structures

It was also desired to develop a method of testing inflatable shell structures in a manner similar to that described above for flexible solid rods. Considerable effort was expended with very little notable success in this quest. However, the experience gained could form the foundation for further work in the area. Primarily, the problems encountered were in the construction of a suitable shell, and in a method to seal and pressurize the shell while subjecting it to the required motion.

The construction problems arose in an attempt to avoid having a stiffened shell. Attempts were made to construct cylinders from polyethylene, polyvinylchloride, and mylar sheet 0.002 to 0.006" in thickness. The difficulties arose at the seam along which the shell was sealed. Several different methods were evaluated as means to effect a pressure tight seal. Any form of solidifying adhesive agent, such as glues, resins or epoxy, was found to be totally unusable. This is evident, since the net effect of these sealers, after they have set, is to impose a non-flexible region in the shell. In addition to grossly distorting the bending or buckling characteristics of the shell, these agents would destroy the homogeniety of the internal weight distribution of the shell, and would produce a distorted centrifugal force pattern upon rotation. Also, such a stiffened band or line would upon bending, either rupture the pressure seal or possibly tear the shell itself.

Chemical agents, producing dissolution of the material itself and a resulting surface to surface bond, were also tried. These proved unsatisfactory, also. Generally, it was very difficult to assure a good pressure seal with this type agent, and if sufficient amounts of material were dissolved to assure a sealed bond, the concentrated mass of the seal line produces the same weight and stiffness problems outlined above.

It was concluded that if non-commerical shells were to be constructed, the sealing agent should be some form of flexible, lightweight adhesive, similar to plastic tape. While not entirely satisfactory, this type agent proved by far the superior of all others evaluated. A tape offers several advantages, in that it is easy to work with, and its inherent flexibility offers the least objectionable degree of stiffening to the shell. Also, a tape generally will be of the same order of magnitude of thickness as the shell, and will produce much less of a weight distribution problem than will be the case for any of the other sealers. A reasonably satisfactory seal was finally achieved on 5 mil mylar, using a double-backed adhesive tape of 2 mil thickness reinforced with a single-backed, nylon-reinforced bonding tape on the outside of the seal line to preserve the pressure seal. Except for the fact that a small area of overlap of the mylar was necessary to effect the seal, there was no noticeable increase in stiffness of the shell walls. The pressure seal was adequate to approximately a 5 psi overpressure (19 psia) and there was no noticeable weight concentration at the seal line. However, as is the case for most plastic adhesives, the seal deteriorated

with time and exposure, and the shell became unusable from a sealing standpoint within 48 hours of its construction. Ideally, work of this type should be done by a facility capable of manufacturing seamless shells, as none of the efforts described herein produced an entirely satisfactory structure.

The second problem area was that of developing a suitable means by which to attach the shell to the testing apparatus, control the incidence angle, rotate the entire structure, and at the same time, either maintain or selectively vary the internal pressurization of the shell. The attachment to the apparatus must be rigid and offer a positive seal for one end of the shell, and, most importantly, must not in any way impede or assist bending or buckling characteristics of the shell. Two designs for a grip mechanism were developed, both of which were workable. The first of these employed a V-groove with an inside milled O-ring groove, the seal being achieved when a matching male V section was pressed into the groove sealing the shell on the inside to the O-ring. This end plate was fastened to a threaded mount which was installed in place of the grip apparatus for the rods described above. While the design of this type of plate is adequate, an excellent job of machining must be done in the manufacture of both the male and female parts of the plate, and the edges are subject to deterioration, lessening the effectiveness of the seal. Consequently, a second design was formulated, employing an extended knife edge and recessed O-ring grooves on a cylindrical plate. External hose clamps are then tightened

over the O-rings, providing the seal, and the extended edge maintains the geometric integrity of the shell and contributes no effects to the bending and/or buckling of the structure. This plate was drilled and tapped to be installed directly onto the testing apparatus, and was equipped with a one-way valve for pressurization and was tapped for installation of a small gage to ascertain internal pressure at the desired instant. From all indications, this final system, given a seamless shell and proper pressurization supply equipment, would allow experimental evaluation of inflatable shell structures. A photograph of the experimental apparatus with one of the mylar shells installed is shown in Figure V-4.

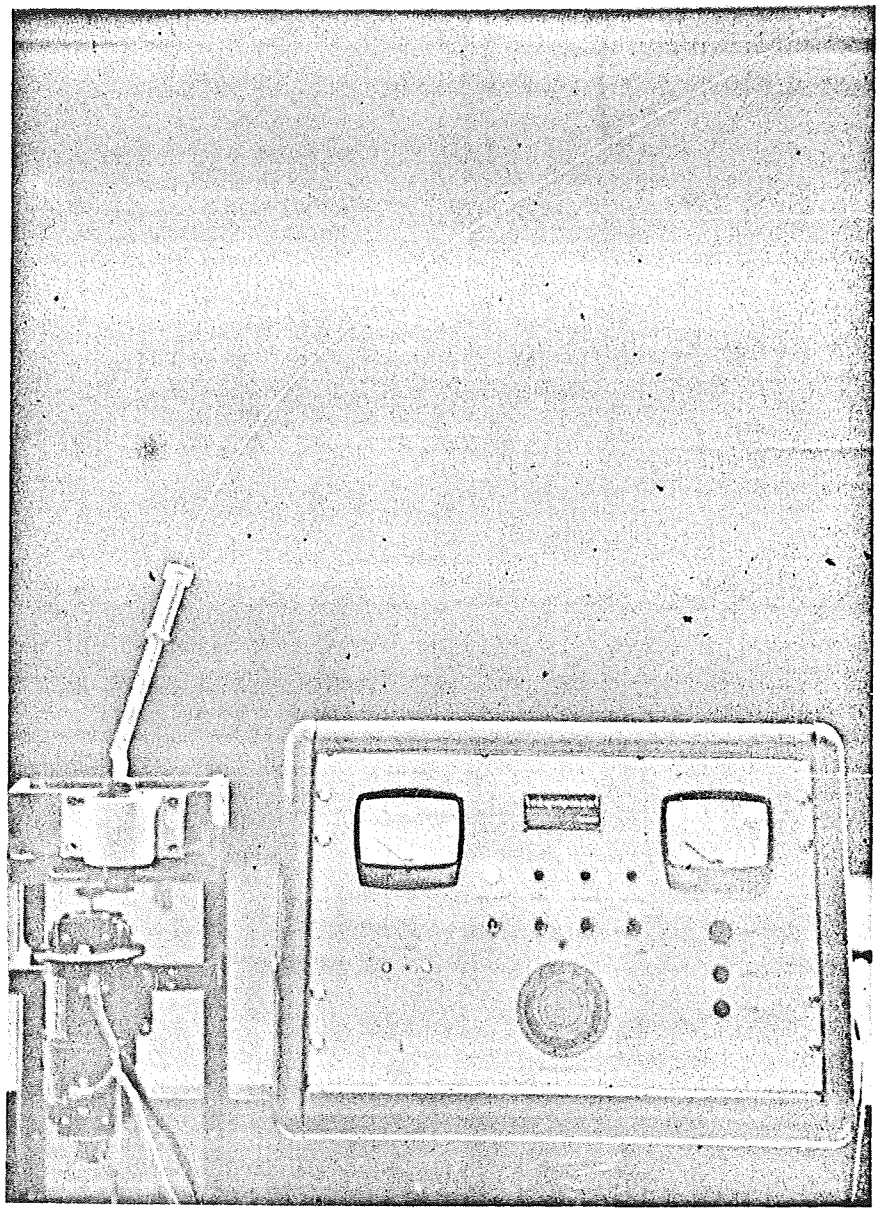

Experimental Apparatus for Testing Slender Flexible Rods

Figure V-1

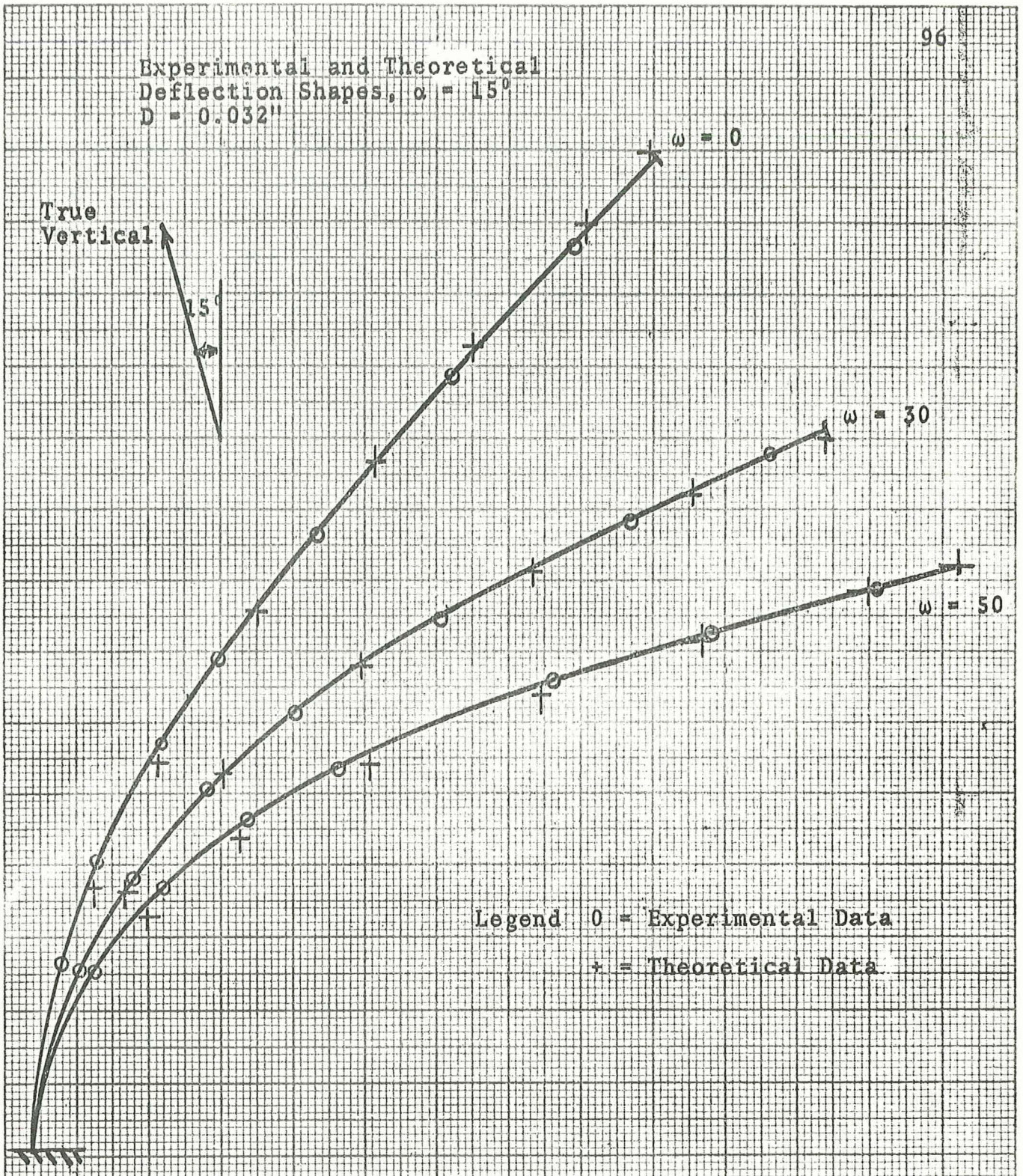
Experimental and Theoretical
Deflection Shapes, α = 15°
D = 0.032"
ω = 0
True
Vertical
15°
ω = 30
ω = 50
Legend 0 = Experimental Data
+ = Theoretical Data

Figure V-2

Experimental and Theoretical
Deflection Shapes, $\alpha = 30^0$
D = 0.032"

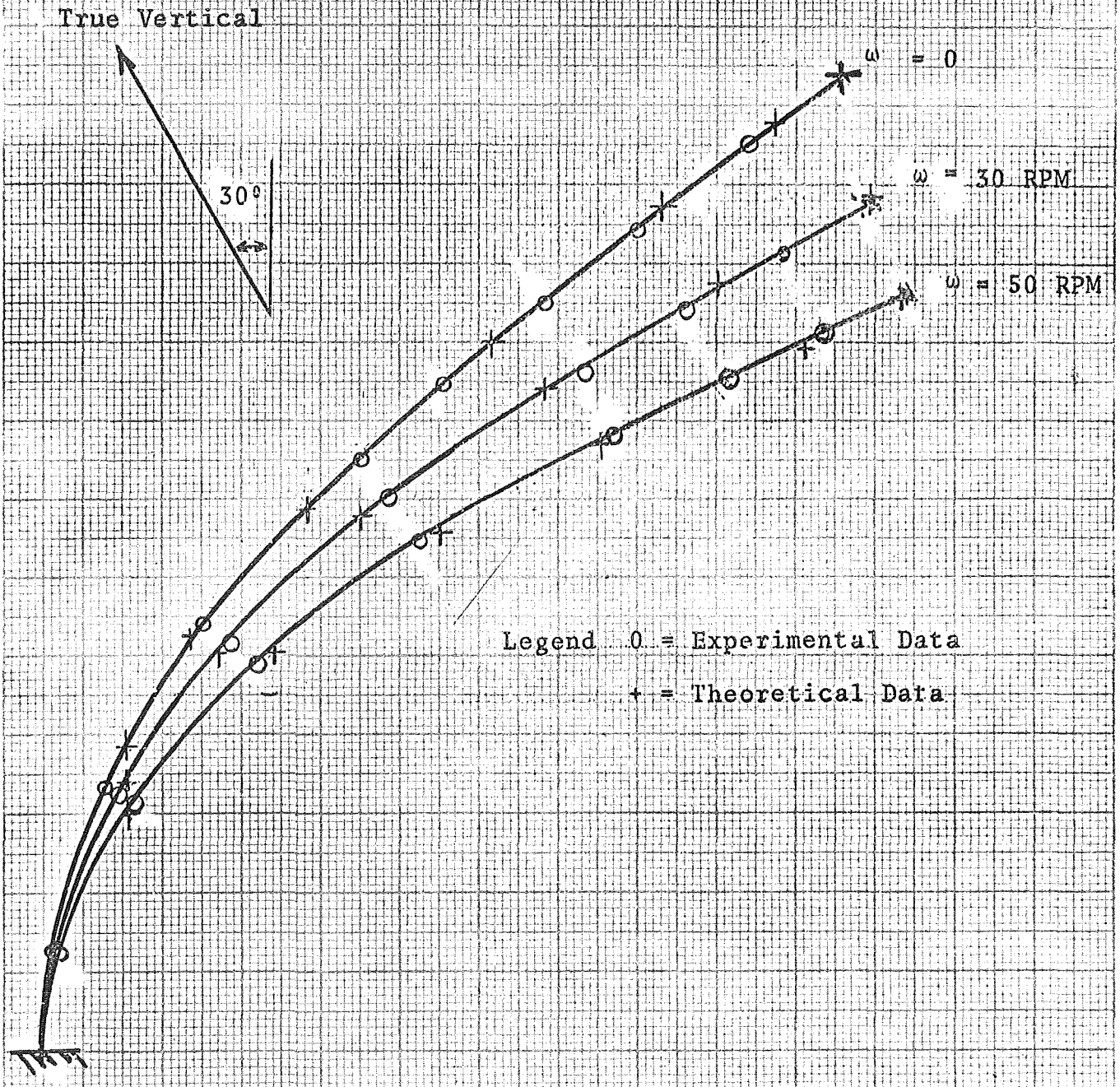

Figure V-3

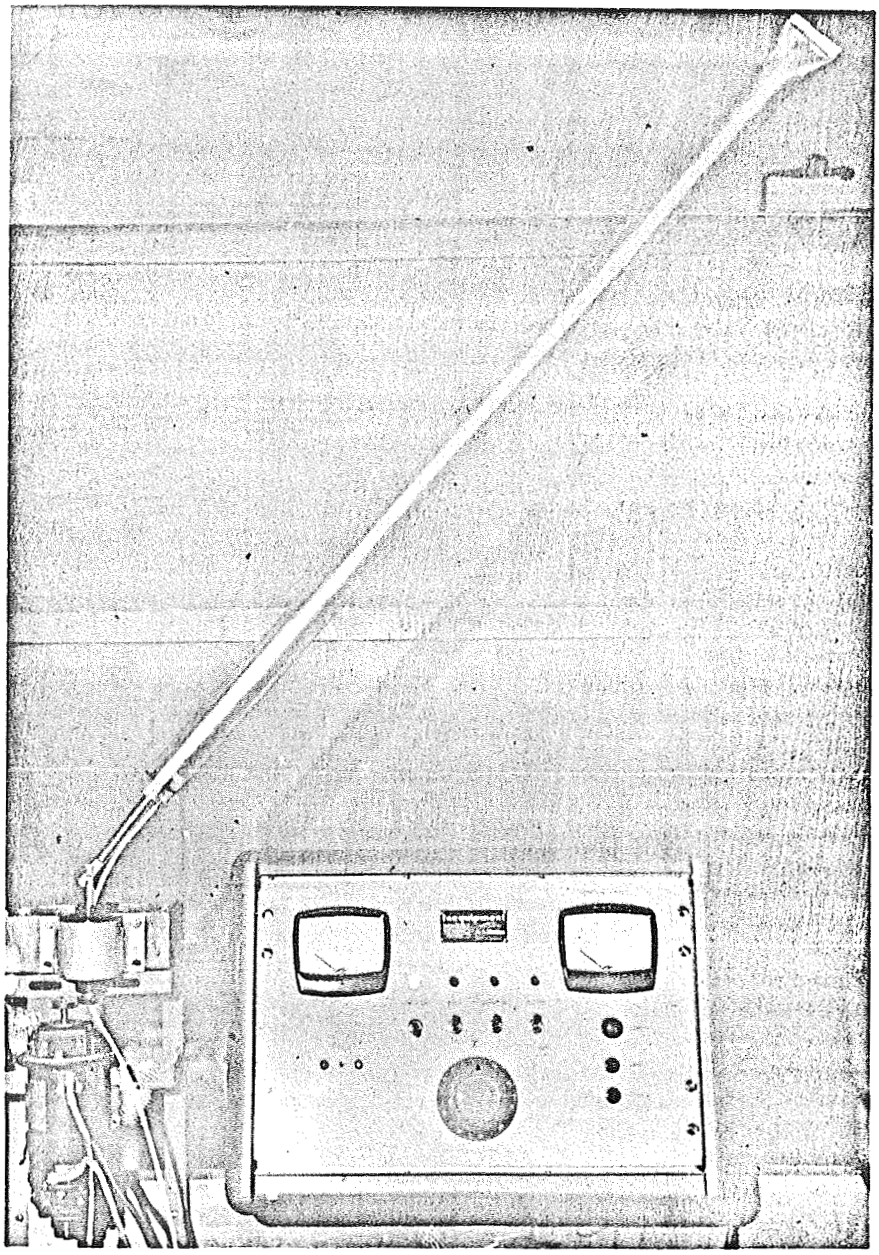

Experimental Apparatus for Testing Inflatable Shell Structures

Figure V-4

Report Distribution

	Code	Quantity
NASA,MSF	PR-SC	1
	MS-IL	1
	MS-T	1
	MS-I	1
	R-AERO-R	12 + repro
Office of Naval Research Research Institute Univ. of Ala. in Huntsville P. O. Box 1247 Huntsville, Ala. 35807	Mr. Bryant Resident Representative	1
University of Alabama:	Director of Contracts and Grants	1
	Bureau of Engineering Research	1

Submitted by Thomas E. Talbert

Leroy E. Wells